Project N. 037110

NEAREST

Integrated observations from NEAR shore sources of Tsunamis: Towards an early warning system

Instrument: STREP

Thematic priority: 1.1.6.3 GOCE (Global Change and Ecosystems)

D6: Crustal geometry, seismic velocity and density models along wide angle profiles

Due date of deliverable: November 2009
Actual submission date: February 2010

Start date of the project: 01/10/2006 Duration: 36 + 6 months

Organisation name of the lead contractor for this deliverable: CSIC

Revision: Final

Project Co founded By the European Commission within the Sixth Framework Programme (2002-2006)		
Dissemination Level		
PU	Public	
PP	Restricted to other programme participants (Including Commission Services)	
RE	Restricted to a group specified by the Consortium (Including Commission Services)	**RE**
CO	Confidential, only for members of the Consortium (Including Commission Services)	

WP2 - Tsunami source characterisation

Task 2.3 – Processing and modelling of wide-angle seismic data

D6: Crustal geometry and seismic velocity along wide-angle seismic profiles

Task 2.3 Leader:

CSIC

Task 2.3 Responsible:

Valentí Sallarès

Unitat de Tecnologia Marina (UTM) - CSIC

Centre Mediterrani d’Investigacions Marines i Ambientals (CMIMA)

Passeig Maritim de la Barceloneta, 37-49
08003 Barcelona, Spain

Authorship

This report has been compiled by Valentí Sallarès and Marc-André Gutscher based on the work made mainly by Audrey Gailler from UBO (data processing and seismic modelling along profile P2) and Sara Martínez from CSIC (data processing and seismic modelling along profile P1). The rest of the persons having contributed are listed in the “Acknowledgements” section, and hereafter referred to as the NEAREST-SEIS working group.

Acknowledgements

Many people have contributed to the outcomes of this report. Obtaining a seismic velocity model such as the ones presented here is a hard task that starts with the design of the cruise, gathering of the necessary instrumentation, obtaining shiptime, preparing, deploying and recovering the Ocean Bottom Instruments, processing the data, and only at the end modelling them. A number of technical and scientific teams have participated in the different steps, and we are deeply grateful to all of them. First, we wish to thank the Captain of R/V Hespérides during the cruise, Pedro Luis de la Puente, as representative of the crew members for their professional work and their cooperative and helpful attitude which ensured successful operation during the cruise and the acquisition of a vast set of high quality oceanographic data. We deeply thank the UTM-CSIC technical team for their efforts, guidance and assistance throughout the data collection, which ensured the high quality of the marine geophysical data collected, and to their main representative J.J. Dañobeitia for his support before and during this cruise. Finally, we acknowledge R. Bartolomé, M. Prada, D. Graindorge, A. Maléndez for their help in diffrerent steps of data processing and modelling. The survey was mainly funded through the Spanish ministry Acciones Complementarias Program (NEAREST-SEIS project, Ref. # CGL2006-27098-E/BTE).

Table of contents

1. Introduction and objectives

This report contains technical information on the data acquired during the NEAREST-SEIS cruise, which started in Cartagena (Spain) on Oct 27th, and finished in Cadiz (Spain), in Nov 13th, 2009, and took place onboard the Spanish R/V BIO-Hesperides, as well as on the seismic velocity models obtained using these data. This NEAREST-SEIS cruise was part of the European Union, FP-6 funded, NEAREST project, concretely of its WP2 "Tsunami Source Characterization". Within the wider framework of NEAREST, the primary objectives of this workpackage and, in particular, of this cruise, are the following ones:

1) to provide information about the crust-mantle boundary geometry and physical properties of the crust beneath the seafloor,
2) to identify the nature of the crust (eg. oceanic, continental or other) and the limits of the different crustal domains in the region based on this information,
3) to obtain information to construct a 3-D P-wave velocity model to be used for improving earthquake locations of seismicity

The cruise was mainly devoted to the acquisition of two wide-angle reflection and refraction seismic (WAS) profiles using a set of 36 Ocean Bottom Seismometers (OBS) (Figure 1).

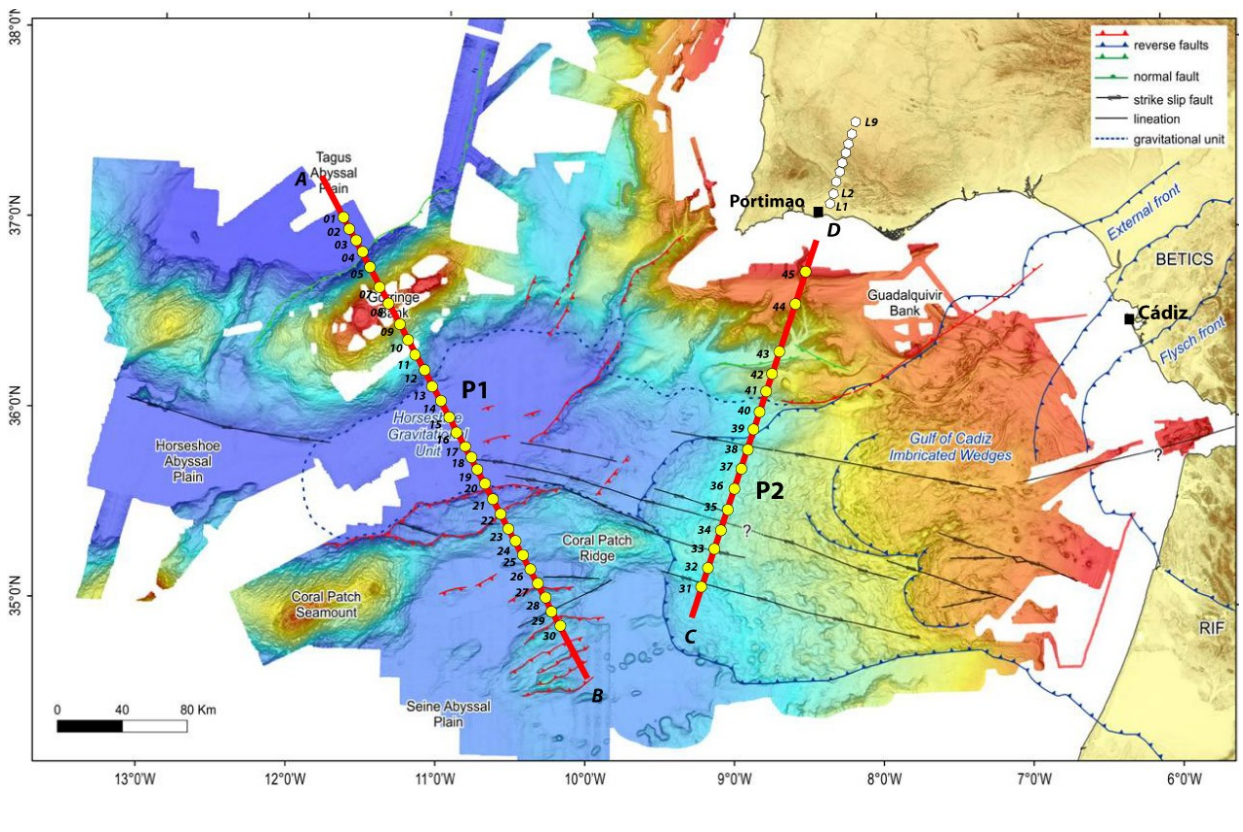

Figure 1. Map showing bathymetric coverage in the Gulf of Cadiz region (SWIM compilation) (Zitellini et al., 2009), with the two profiles acquired during the Nearest-Seis cruise superimposed in red. Yellow circles with numbers indicate OBS locations.

- 30 OBS were deployed along profile P1, which is 365 km-long and extends from the

Tagus Abyssal Plain, over Gorringe Bank, across the Horseshoe Abyssal Plain and the Horseshoe fault, up onto Coral Patch Ridge and finally to the fold and thrust belt in the Seine Abyssal Plain beyond the NW Moroccan continental margin.

- 15 OBS and 7 landstations were deployed along P2, which is 257-km-long and crosses from the Easternmost Seine Abyssal Plain (just beyond the NW Moroccan margin) crosses the accretionary wedge and several of the “SWIM” lineaments (including the buried prolongation of Coral Patch Ridge), then the Guadalquivir Ridge/Portimao Bank structure, the Portimao Canyon and all the way up onto the S. Portuguese continental shelf.

This report is structured as follows: first, we present the list of participating institutions (section 2). Then, we make an overview of the geologic and tectonic setting of the NW Iberian margin in section 3. In section 4, we present the data acquired and the processing applied. In section 5 we explain the methodology used to model the data together with the inversion strategy followed to construct the models, and in section 6 we summarize the main results. In section 7 we present the uncertainty analysis made for profile P2. The results obtained along P2 are complete and almost final, whereas there is still work to do in P1, specially concerning the uncertainty analysis. Gravity modelling along both profiles is being done at present day and therefore it is not included in this report.

2. Participating institutions

UTM-CSIC

Unitat de Tecnología Marina - CSIC

Centre Mediterrani d'Investigacions Marines i Ambientals

Passeig Marítim de la Barceloneta, 37-49

08003 Barcelona (Spain)

UBO-IUEM

Universite de Bretagne Occidentale

Institut Universitaire Europeen de la Mer

UMR 6538 Domaines oceaniques

Place N. Copernic

29280 Plouzané (France)

IFREMER

Institut français de recherche pour l'exploitation de la mer

Place N. Copernic

29280 Plouzané (France)

Universidade de Lisboa

Fundacao da Faculdade de Ciencias da Univ. de Lisboa

Centro de Geofisica da Universidade de Lisboa

Campo Grande, Ed. C8, piso 6

1749-016 Lisboa (Portugal)

ICTJA-CSIC

Institute of Earth SciencesJaume Almera- CSIC

Lluis Solé i Sabarís, s/n

08028 Barcelona (Spain)

3. Geological setting of the SW Iberian margin

The region offshore SW Iberia lies at the eastern end of the so called Azores-Gibraltar transform, and is part of a complex plate boundary between the African (Nubian) and Eurasian plates (Figure 2). The tectonic history of this area has been dominated by the long-term evolution of the triple junction, between the North American, African and Eurasian plates, as well as the interaction, with other smaller blocks, e.g. the Iberian plate (Srivastava et al., 1990). Here, a major limit exists, between the Central Atlantic domain, which opened in the late Triassic earliest Jurassic, and the Northern Atlantic domain, which opened in the Cretaceous (Roest and Srivastava, 1991; Olivet, 1996; Gracia et al., 2003a; Sahabi et al., 2004). The modern day plate boundary in the Gulf of Cadiz is fairly diffuse, marked by an E-W trending band of seismicity about 100-200 km wide (in a N-S direction) (Buforn et al., 1988; 1995; Stich et al., 2003;2006; Gutscher et al., 2009a). Moderate to strong earthquakes have struck here in the past (1964 Huelva earthquake M6.5; 1969 Cape St. Vincent earthquake M7.9, and 2007 Horseshoe earthquake M6.1), with mostly compressional and strike-slip focal mechanisms (Stich et al., 2003; 2006). Plate kinematic models and GPS observations are in good agreement that NW Africa (Nubia) is moving in a NW to WNW direction with respect to Iberia at a velocity of approximately 4mm/yr (Argus et al., 1989; DeMets et al., 1994, McClusky et al., 2003, Nocquet and Calais, 2004).

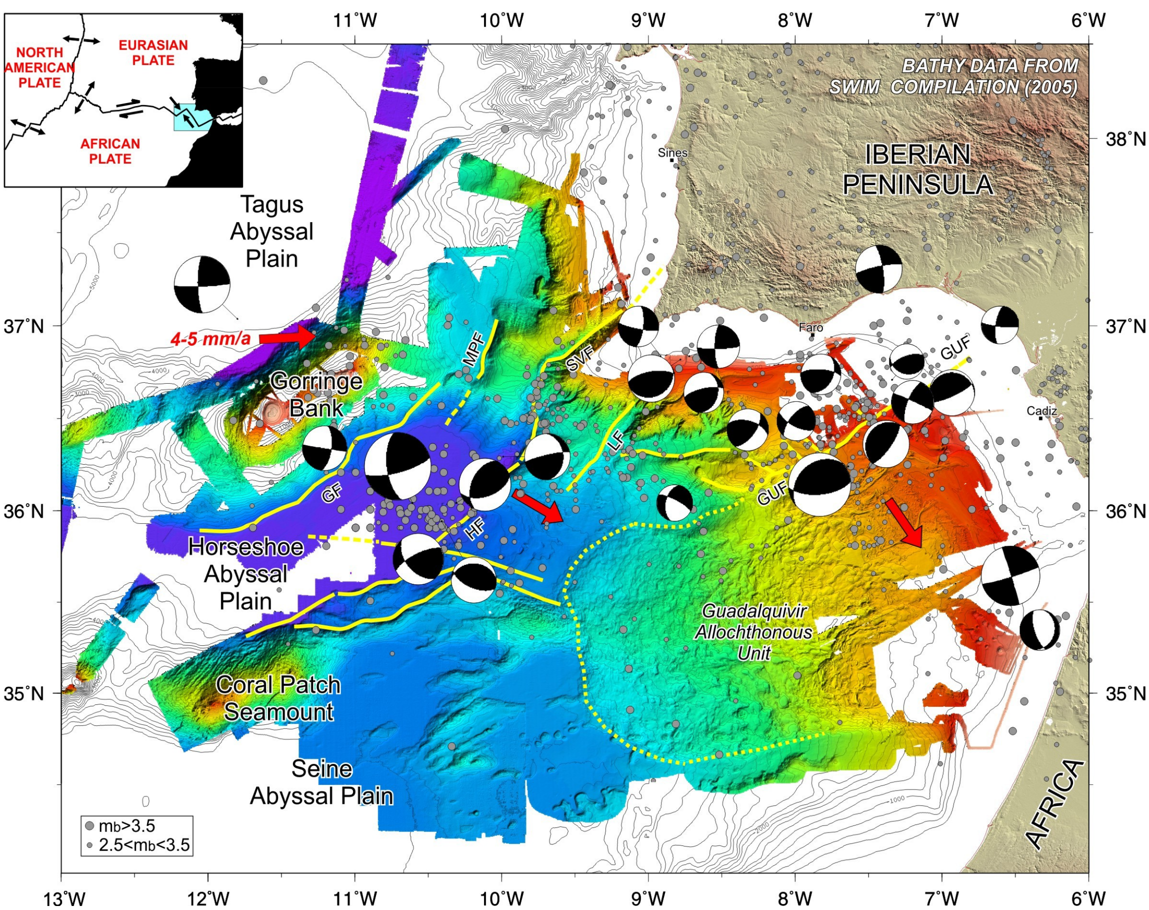

Figure 2.- Inset: Plate tectonic setting of the SW Iberian Margin along the boundary between the Eurasian and African Plates. Detailed swath-bathymetric map of the Gulf of Cadiz from the EuroMargins SWIM compilation (Zitellini et al., 2009). Seismicity from the "Instituto Geográfico Nacional" catalog for the period between 1965 and 2000 is depicted (I.G.N., 1999). Small grey dots are epicentres of earthquakes for 2.5 <mb <3.5, and large grey dots for earthquakes of mb >3.5. Fault plane solutions are from Stich et al. (2005). Red arrows show the direction of plate convergence from NUVEL1 model (Argus et al., 1989). Physiographic domains of Gulf of Cadiz and main active faults (thick yellow lines) are located. GF: Gorringe Fault; MPF: Marques de Pombal Fault; HF: Horseshoe Fault; SVF: Sao Vicente Canyon Fault; LF: Lagos Fault; GUF: Guadalquivir Fault.

As stated in the introduction, given the complex tectonic history of the region and the ongoing, seismic activity, the two primary objectives of the NEAREST-SEIS survey were: to probe the deep structure of the Southwest Iberia margin and adjacent oceanic areas, in order to characterize the nature of the crust, and to identify the major modern day discontinuities and the limits between the major geologic domains, which may be expressions of major faults.

SW Iberia has been struck by strong historical seismicity, most notably the catastrophic Great Lisbon earthquake of 1 November 1755. This event with an estimated magnitude 8.7, destroyed the city of Lisbon, and cities along the southern Algarve coast of Portugal, and along the coasts of SW Spain (Cadiz, Huelva) and NW Morocco, causing an estimated 60,000 deaths (Martinez-Solares et al., 1979; Johnston, 1996; Baptista et al., 1998a). This earthquake is the greatest recorded in European history and was felt as far away as Hamburg and the Azores. However, the complex regional tectonics and the diffuse nature of the plate boundary, makes it difficult to identify the principal faults which store and release the greatest seismic moment over the long term. Therefore, the source region of the 1755 earthquake remains a subject of lively debate, and numerous candidate fault zones have been proposed by different authors (Johnston, 1996; Baptista et al., 1998b; Gracia et al., 2003b; Terrinha et al., 2003; Vilanova et al., 2003; Gutscher, 2004; Stich et al., 2007; Barkan et al., 2009; Gutscher et al., 2009a). The tsunami triggered by the 1755 earthquake devastated port regions in the SW Iberia - NW Morocco region with observed waves of 5-15 m height (Baptista et al., 1998a). This tsunami whose impact was also felt in the Antilles, remains the largest tsunami ever observed in the Atlantic (Barkan et al., 2009).

3.1. The origin of the margins of SW Iberia and NW Africa

The study area is located at the intersection of two continental margin "corners". The corner of the NW African margin developed during Triassic-Jurassic times as the Central Atlantic formed by the rifting of Africa from North America. The NW Moroccan margin was situated at the southern end of the modern day Grand Banks of Newfoundland and formed by sub-normal extension along a N60 trending fault and by transcurrent motion along the Southern Grand Banks fault (today oriented N120) (Stampfli et al., 2003; Sahabi et al., 2004). The SW corner of the Iberian continental domain represents the intersection of a N-S trending margin, between Iberia and the Flemish Cap - Grand Banks Margin of Newfoundland (Canada), and the Southern Grand Banks transform metioned above (Roest and Srivastava, 1991). The oceanic domain in the Gulf of Cadiz in between these two continental corners was first structured by this transcurrent motion. Later this domain may have been the site of minor amounts of seafloor spreading (possibly SE-NW) which could have opened a narrow oceanic corridor separating southern Iberia from NW Africa. Further east this oceanic domain widens to become the Tethys separating Gondwana from Eurasia .

The exact nature of the basement in the deep oceanic domains offshore SW Iberia (Tagus Abyssal Plain, Horseshoe Abyssal Plain, Seine Abyssal Plain) is unknown and difficult to determine for two reasons. 1) There are few recognizable magnetic anomaly patterns (Figure 3), and 2) the seafloor is covered by a roughly 2-4 km thick layer of Mesozoic to recent sediments. Thus basement samples are not easy to obtain. The only deep sea drilling in the region which penetrated to basement were; DSDP site 120 on Gorringe Bank, where serpentinized mantle has also been recovered directly at the seafloor during deep-sea submersible expeditions (Lagabrielle and other references) and off the western Moroccan margin (at the foot of the Mazagan plateau - near present day El Jadida) at ODP site 546 during Leg XX drilling (Hinz et al., 1982). DSDP hole 135 penetrated Jurassic sediments but did not reach basement.

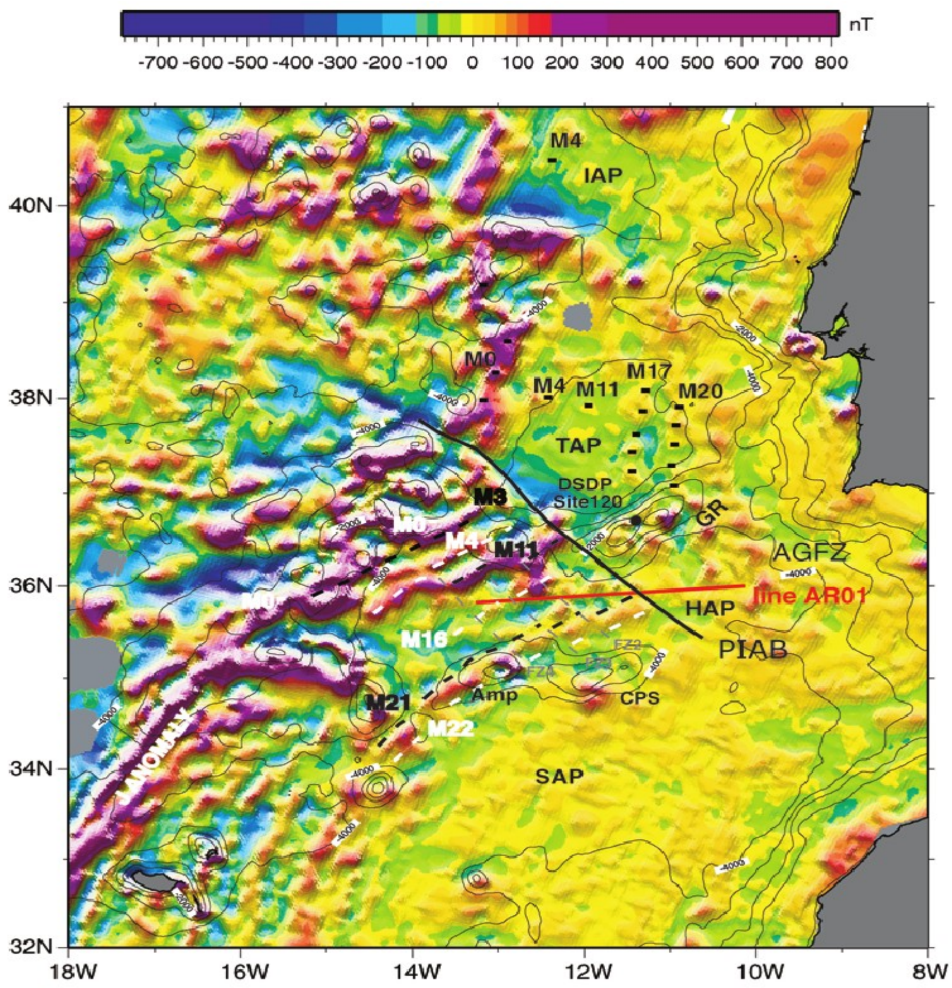

Figure 3.- Marine magnetic anomalies of the eastern Atlantic ocean offshore southwest Iberia and northwest African margins (from Rovere et al., 2004) Outlined seafloor topography from satellite altimetry (Smith & Sandwell 1997). Iberia Abyssal Plain (IAP); Tagus Abyssal Plain (TAP); Horseshoe Abyssal Plain (HAP); Gorringe Ridge (GR), Ampère Seamount (Amp), Coral Patch Seamount (CPS),

Azores–Gibraltar Fracture Zone (AGFZ), Seine Abyssal Plain (SAP). Interpretation of the magnetic anomalies based on Roest et al. (1992) and Srivastava et al. (2000). Inferred Palaeo Iberia–Africa Plate Boundary (PIAB) during the opening of the Central Atlantic ocean. The boundary ends near M0, the youngest constrained anomaly.

Because of the lack of basement samples, current knowledge of the crustal domains in the NEAREST study area is based almost exclusively on seismic data. Using available multi-channel and wide-angle seismic data, compilations of depth to basement and sediment thickness maps were established (Figure 4). These compilations confirm the generally thick sedimentary cover and highlight the eastward increase in sediment thickness in the Gulf of Cadiz related to the sedimentary wedge. They also indicate an E-W trending trough in depth to basement and crustal thickness. On the basis of crustal thickness and some E-W trending magnetic lineations Verhoef et al., 1991), it seems possible that oceanic crust may extend into the Gulf of Cadiz region. The current OBS survey should help to resolve this question.

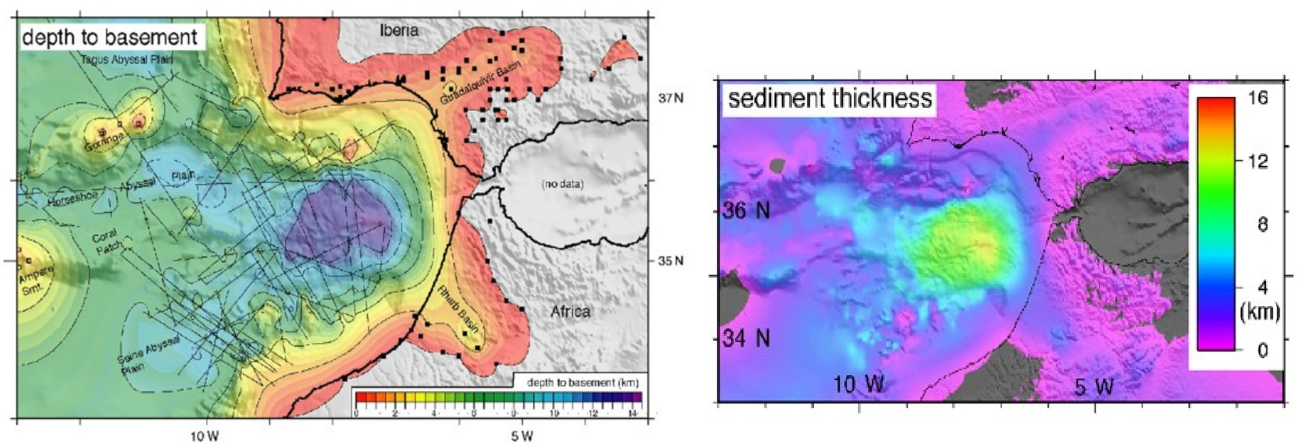

Figure 4.- Structural maps of the S. Iberian/N. Moroccan region. Left: depth to basement map obtained from joint interpretation of all seismic profiles shown (Thiebot and Gutscher, 2006); Right: sediment thickness map obtained by combining relief (adding topography and subtracting bathymetry) with the depth to basement map. The figures are from Gutscher et al. (2009).

3.2. Scientific rationale of the wide-angle seismic profiles P1 and P2

Wide-angle seismic profile P1 runs NW-SE from the Tagus Abyssal plain to the Seine Abyssal plain crossing the Gorringe Bank, the Horseshoe Abyssal plain, and the Coral Patch ridge. The main objective of this line are to determine the deep structure and nature of the basement at the different geologic domains, in order to better understand the general geodynamic evolution of the Eurasia-Nubia compressive setting, as well as the deep geometry of the main décollement surfaces across these tectonic limits, which might be potentially associated with seismogenic/tsunamigenic faults (especially the Gorringe Bank and the Coral patch ridge).

Wide-angle seismic profile P2 begins in the Easternmost Seine Abyssal Plain (just beyond the

NW Moroccan margin) crosses the accretionary wedge and several of the “SWIM” lineaments (including the buried prolongation of Coral Patch Ridge), then the Guadalquivir Ridge/Portimao Bank structure, the Portimao Canyon and continues all the way up onto the S. Portuguese continental shelf and onto the oshore Variscan continental domain of Southwest Iberia. The primary objectives of this line was to obtain information on the crustal nature and overall geometry (thickness, dip, etc.) across these major structures and tectonic boundaries,and to reveal the geometry of the continent-ocean boundary at the SW Iberian margin.

4. Wide-angle seismic data set

The wide-angle seismic data acquired along profiles P1 and P2 with the B/O Hesperides during the NEAREST-SEIS cruise is presented here. The source used was composed of 7 airguns (model 1500LL) organized in two arrays, providing a total volume of 4520-in^3 (Figure 5).The airguns were tuned to the first bubble to enhance deep frequencies and ensure a good penetration (Avedik et al., 1993), and the shot interval was set at a time of 90-s leading to a ~210-m shot spacing.

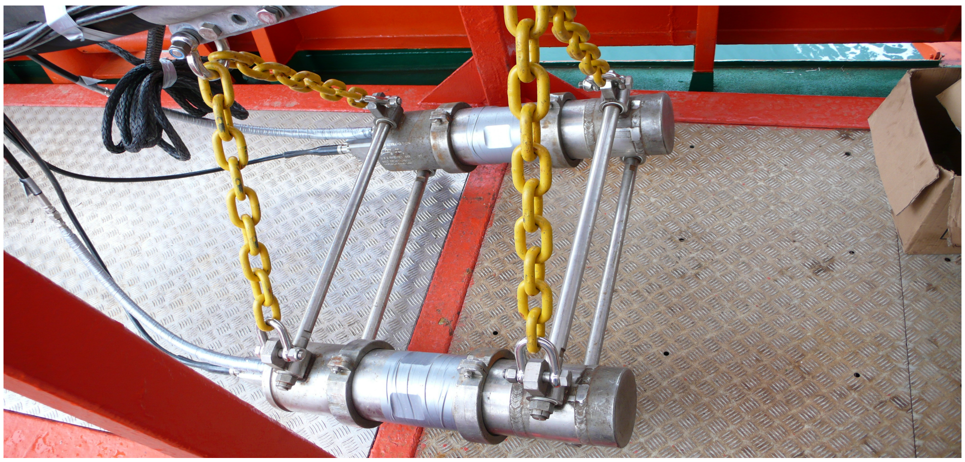

Figure 5.- Detail of a two Bolt 1500LL airgun cluster used in the Nearest-Seis airgun array.

Pre-processing of the OBS data included calculation of the clock-drift corrections to adjust the clock in each instrument to the GPS base time and instrument locations were corrected for drift from the deployment position during their descent to the sea-floor using the direct water wave arrival. For that we used a home-made script based on a grid-search algorithm at increasing spatial resolution using the detailed multibneam bathymetry available in the area (see Figure 1). Figure 6 shows an example of the OBS locations obtained before and after the re-location processes, as well as its uncertainty. Typically, the difference between the expected and actual OBS locations is of the order of a few hundreds of meters.

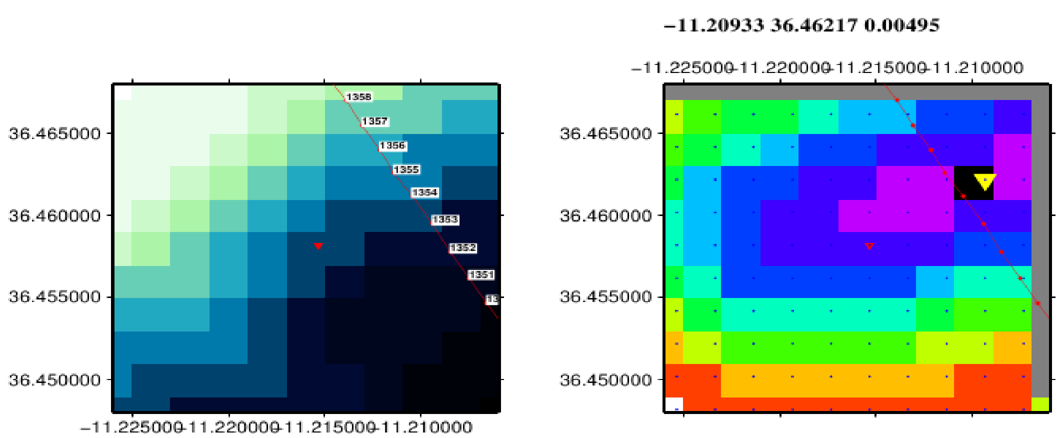

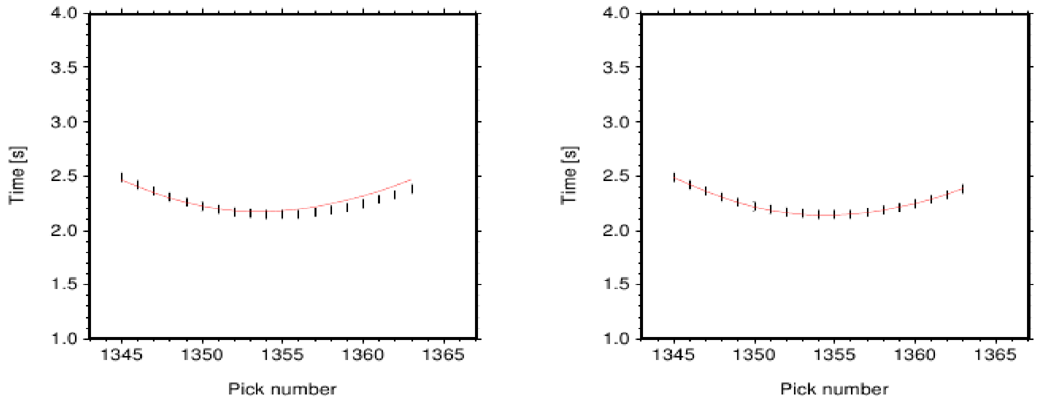

Figure 6.- Four panels showing the relocation process. Upper left show bathymetry, shotpoints and OBS deployment location (red triangle). Upper right show shot line, deployment location and relocated position (white triangle). Couloring is proportional to water wave rms of different locations. The bottom panels show traveltime fitting of water wave for the deployment (left) and relocated positions (right).

The seismic records were further pre-processed by applying Automatic Gain Control, whitening (a predictive deconvolution), as well as a band-pass filtering of 5-20 Hz. The different panels of Figure 7 correspond to the seismic data recorded at OBS deployed along profile P1, whereas those of Figure 8 are record sections at OBS and landstations deployed along P2. Most of the wide-angle data are of good quality, showing clear phases refracted at the sediments (Ps), and basement (Pb) up to more 100 km offset in some areas. Ps is clear in almost all record sections, but the Pb change significantly in the different regions. In some regions, Pb clearly correspond to a seimsic phase refracted at a oceanic-like crust (Pg), but in other regions, Pb shows apparent velocity that is much higher than that of a crust, indicating that it is probably a mantle refraction (Pn). Apart from the diffrerent refracted phases most record sections show clear reflections at the base of the sedimentary layer(s) (PsP) and several ones show reflections at the crust-mantle boundary (i.e. Moho reflections, PmP)

In P1, the OBSs showing the longests offsets are those located at the Tagus Abyssal plain (TAP), where seismic phases are clearly identified at distances over 150 km (Figure 7a). The maximum offset is smaller in the OBS located in the Gorringe bank (GB), Horseshoe and Seine Abyssal plains (HAP and SAP, respectively), where it rarely exceeds 80-90 km (Figure 7b, 7c and 7d). It is probably related to the nature of the seafloor, rather unconsolidated, gravitational unit in HAP, and rough topography in SAP. At short offsets, all the record sections show clear PsP phases. In TAP and SAP, there is only one single, low-velocity phase (Figure 7e), whereas in GB and HAP there are two different sedientary phases that correspond to the upper (gravitational unit) and lower (Mesozoic sediments) levels (Figure 7f). SAP is the only place where a clear

In P2, significant variations are observed between record sections of instruments located southward on top of the accretionnary wedge frontal part and instruments located northward in the Algarve basin area and on-land (Figure 8a and 8b). This is probably related partly to the strong change in the bathymetry (~3000 m) across the Gulf but also to a strong lateral variation in the crustal structure along the profile. Seismic sections from OBS located close to the Portimao canyon in very shallow water show weak information. On the other hand, far offset PmP and Pn phases can be traced without ambiguity on land-stations data (Figure 8c). Instruments located southward in deeper water show clear arrivals, with high amplitude reflections at the sediments-crust boundary (Ps and PsP) (Figure 8d) and crustal arrival velocities reaching up to 7.0 km/s (Figure 8e). From the 7 land-stations records available, only the three located the closest to the coast were used in the modelling.

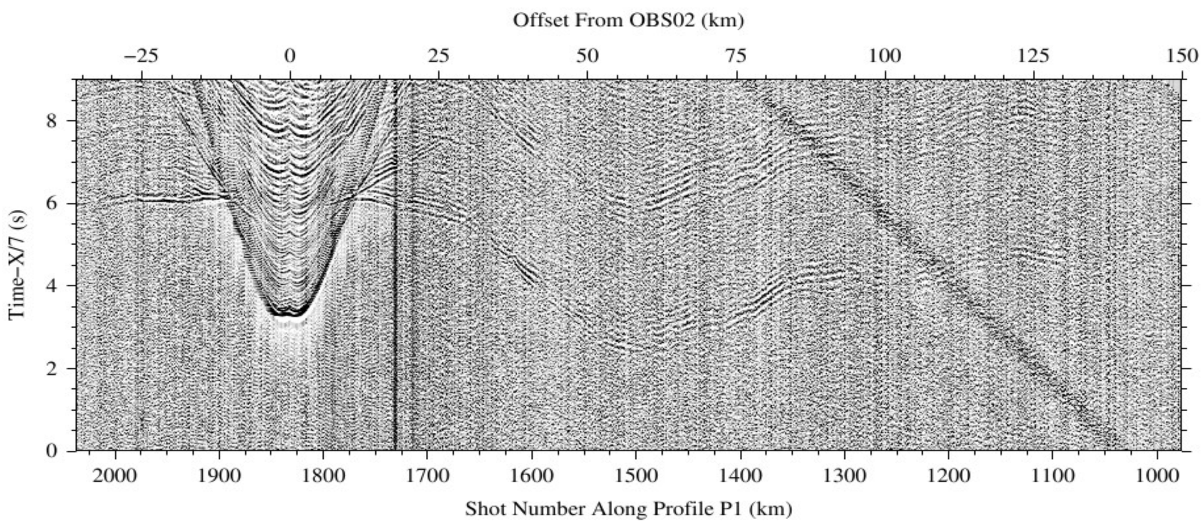

Figure 7a

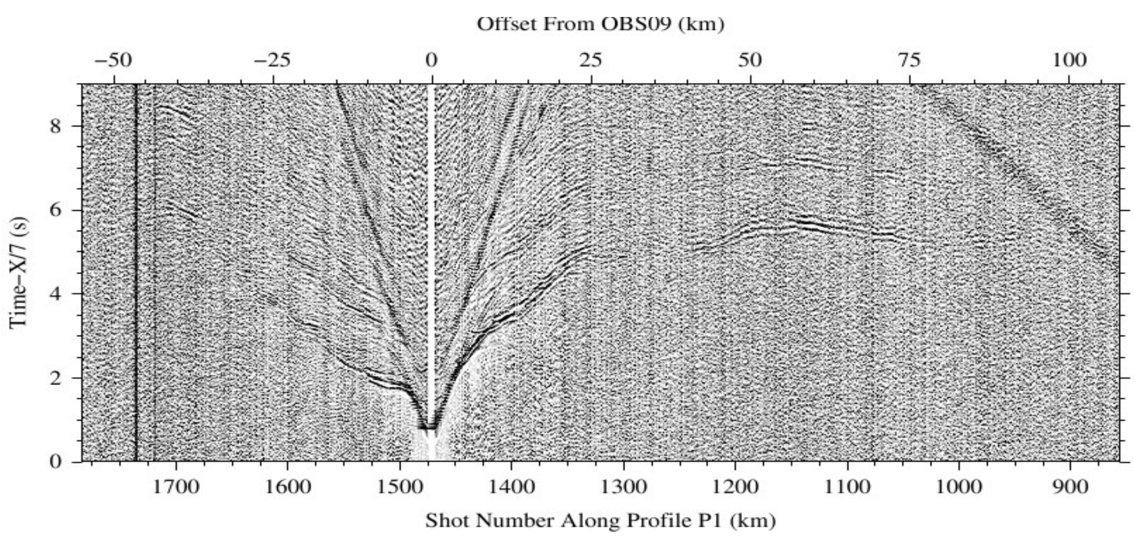

Figure 7b

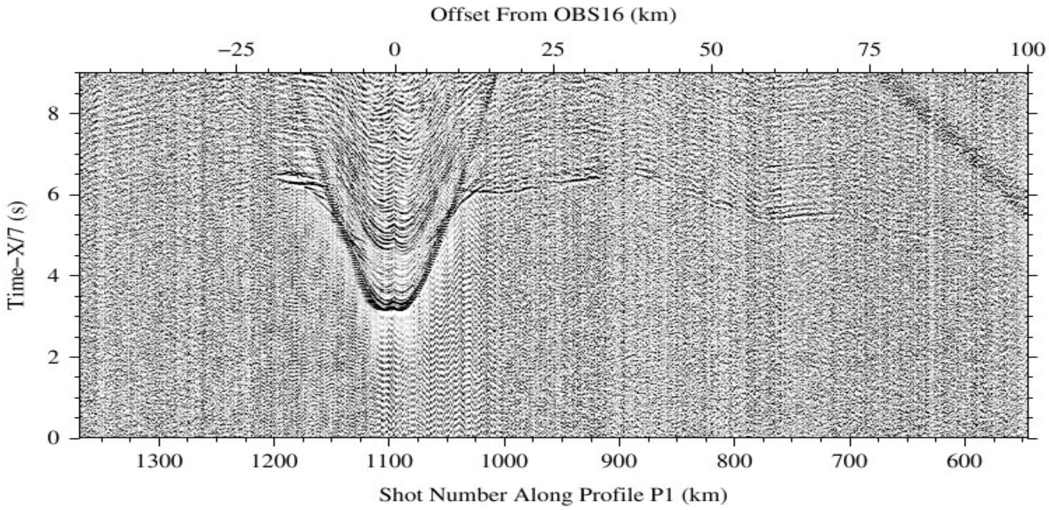

Figure 7c

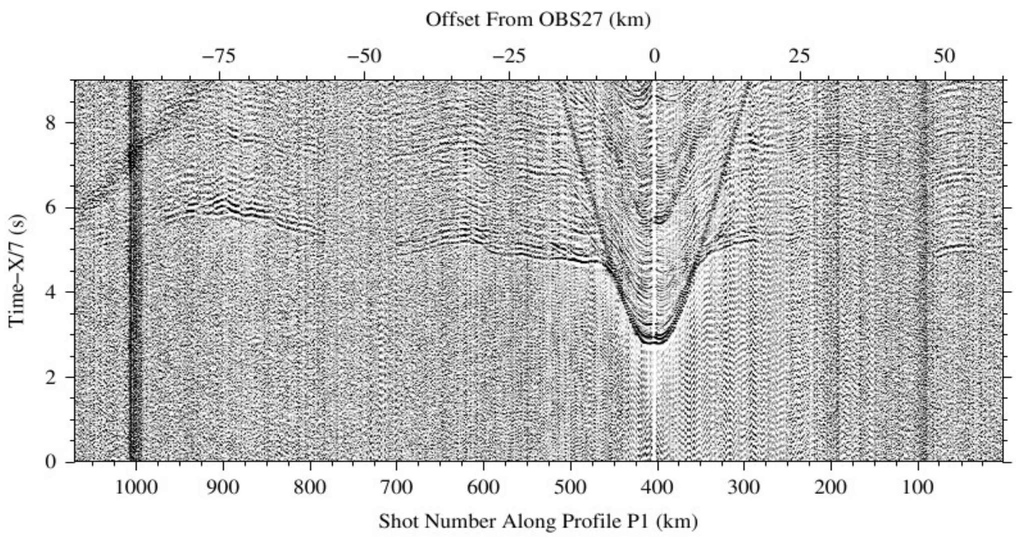

Figure 7d

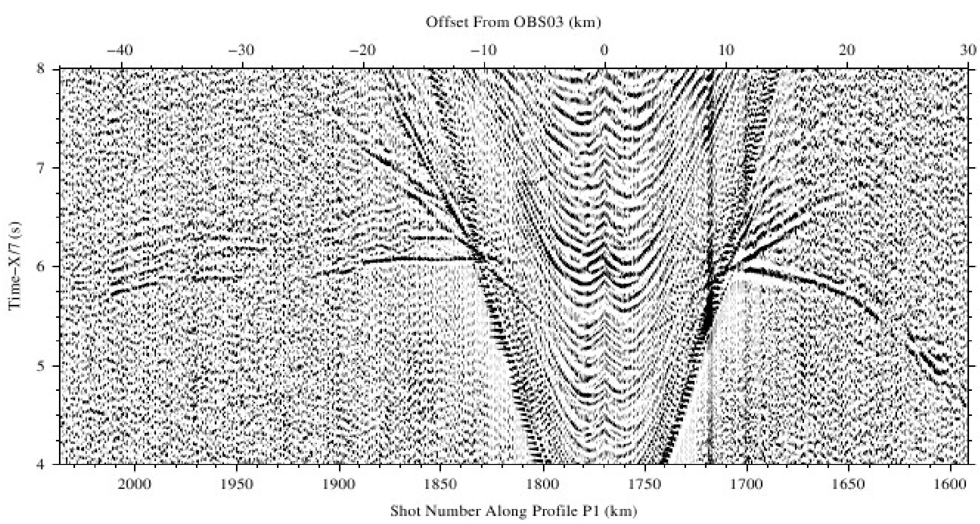

Figure 7e

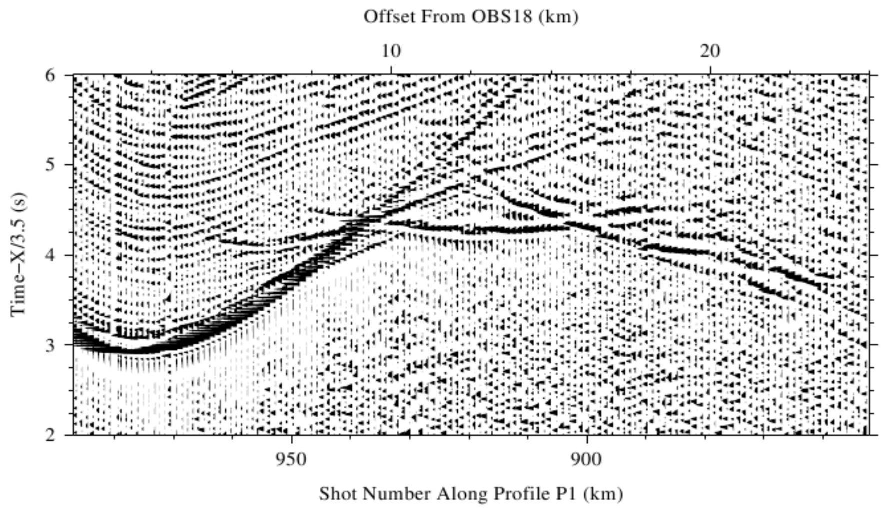

Figure 7f

Figure 7.- Record sections sponding to different OBS. For the particular locations of the different instruments see Figure 1.

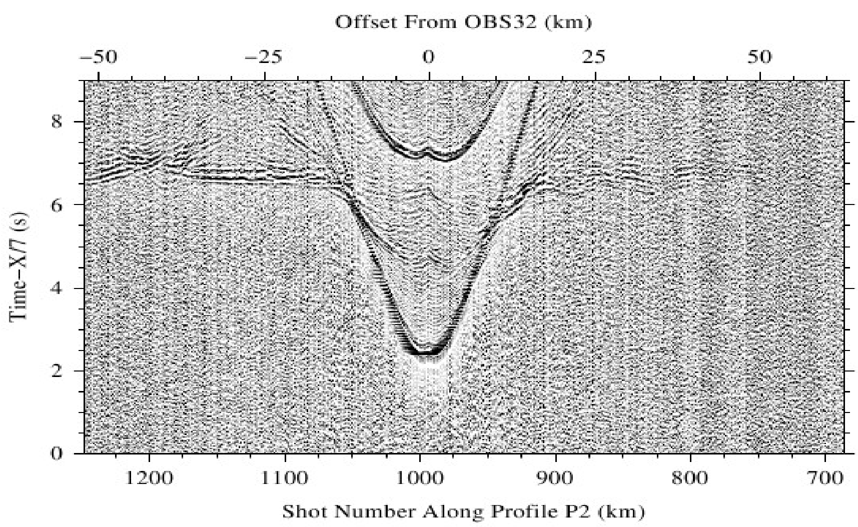

Figure 8a

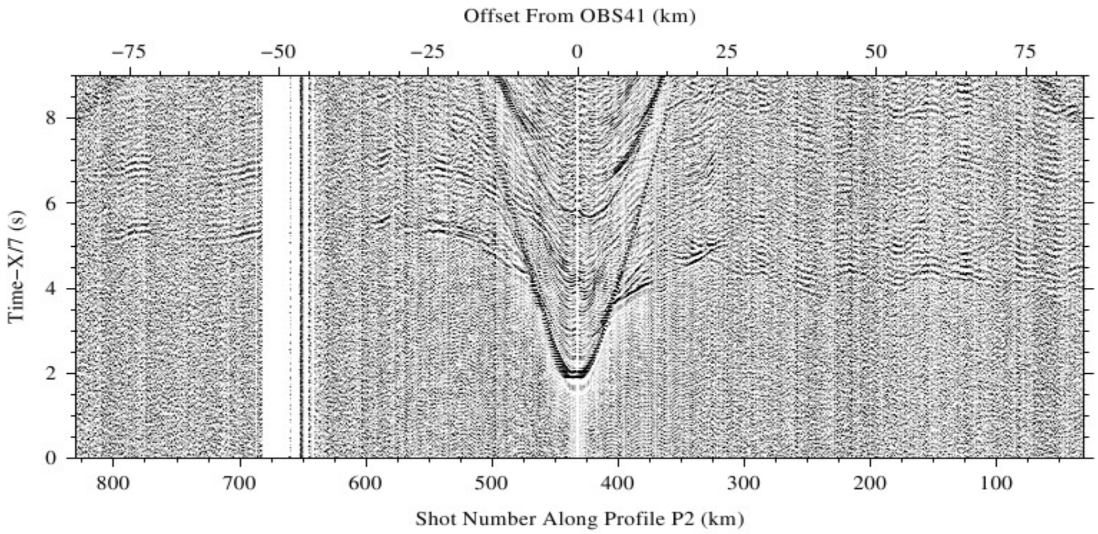

Figure 8b

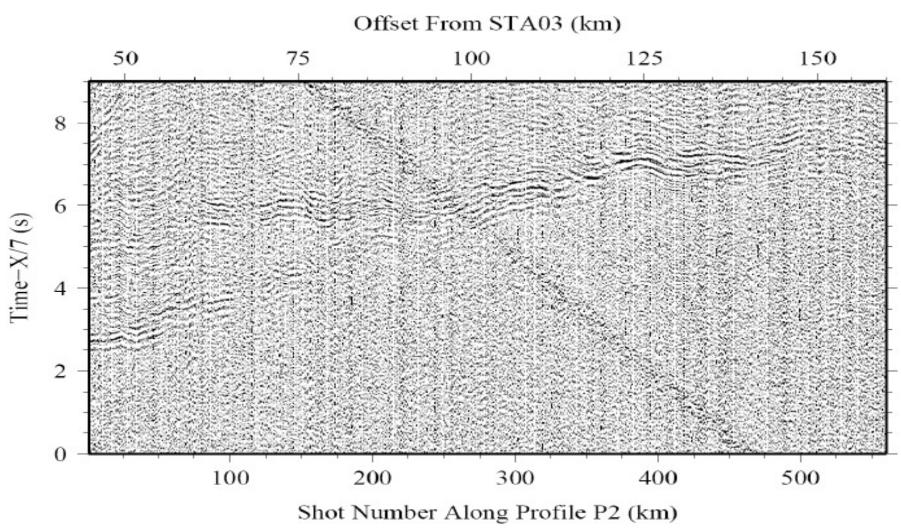

Figure 8c

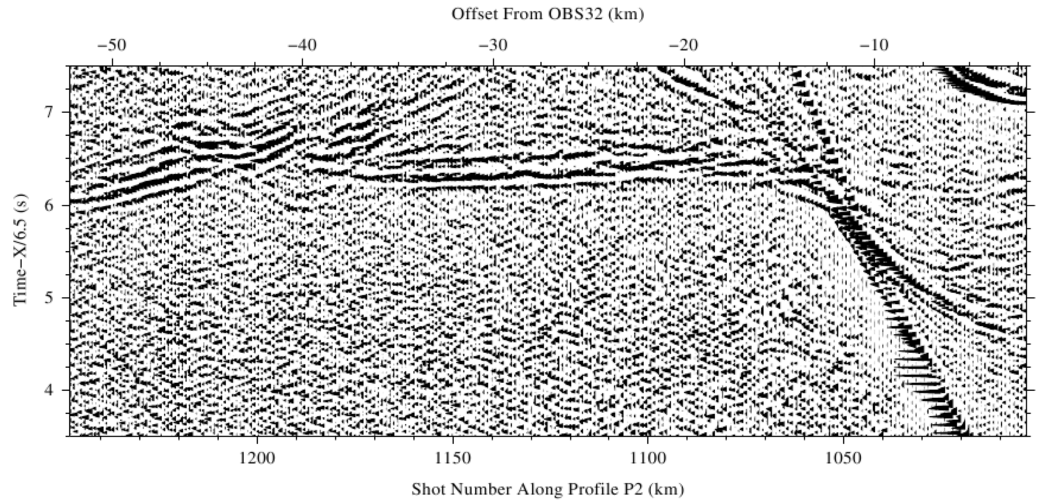

Figure 8d

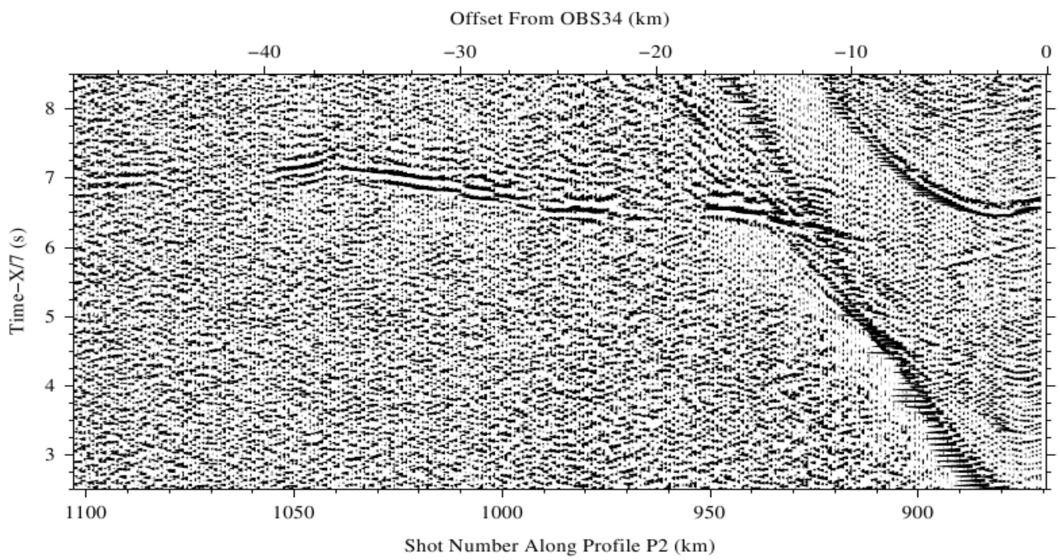

Figure 8e

Figure 8.- Record sections of OBS located along profile P2. For OBS location see figure 1.

5. Traveltime picking and seismic velocity modelling

5.1. Inversion technique and strategy

First arrival travel times (Ps and Pb -either Pg or Pn-), PsP and PmP reflections and the Pn phases were identified in the record sections. Picking was done manually on unfiltered data where possible and if necessary a whitening, a butterworth filter (5-20 Hz) and an AGC were used. PmP and Pn arrivals could not be identified on all the record sections, especially for shallow water instruments. Ps phases are observed and picked on OBS data located in the southern part of the P2 profile (OBS 31 to 38 + negative offsets of OBS 39 to 43) only. The estimated picking error takes into account the quality of the phase and a possible systematic shift in the arrival identification in order to weight the different picks during inversion. A 40-50 ms and 60-70 ms picking error was assigned respectively to near offsets and far offsets Pg arrivals. A 60 and 90 ms error was assumed for Ps and Pn phases respectively, and 100 ms for PmP phases.

The 2D velocity-depth model was derived using the joint refraction and reflection travel time tomography method developed by Korenaga et al. (2000). This method allows inverting simultaneously and independently first arrival travel times (refracted phases) and a reflection phase, to produce respectively a smooth velocity model and the geometry of a reflector. Traveltimes and ray paths are calculated using a hybrid ray-tracing scheme based on the graph method and the local ray bending-refinement (van Avendonk et al., 1998). Smoothing constraints from predefined correlation lengths and optimized damping for the model parameters are used to regularize an iterative linearized inversion (see Korenaga et al., 2000 for more details).

A preliminary inversion was performed in both P1 and P2 profiles using the entire data set, including Pg, Pb and PmP phases to invert for the velocity field and the geometry of the crust-mantle boundary along the whole profile (the 2D starting velocity model being generated from a 1D reference velocity model that best fits the bathymetry-corrected traveltimes of Pg and Pn arrivals). The resulting model (not shown) along P2 revealed complex crustal structure variations and a sharp change in the Moho geometry that could not be taken into account properly through this global inversion and associated parameterization. Moreover, information given by the Ps refracted phases could not be added with such an inversion procedure.

That’s why the final velocity model proposed here and shown as final results in the next section was constructed for both P1 and P2 using a hybrid approach of multistep, layer-stripping tomography. The data were split into different parts in accordance with the variations observed between record sections of instruments located on top of the accretionnary wedge frontal part and instruments located in the Algarve basin area and on-land for P2 and for the OBS located at TAP and GB, HAP, and SAP in the case of P1. In the case of P2 the results obtained are almost final, and all the procedure was applied to the whole data set, but in the case of P1 the results shown are still preliminary and out team is presently working to refine them, specially at the deepest part. This is the reason why uncertainty analysis is still to be made in P1. We will thus first present here the results obtained in the different steps of the inversion procedure for P2, and then for P1.

5.2. Profile P2

The intermediate velocity model for the south part of the profile (south intermediate velocity model) was constructed using two layers: (1) sediments and (2) crust. The sediment refracted Ps and reflected PsP phases were used to invert for the velocities and thickness of the accretionnary wedge sedimentary cover, and hence the geometry of the sediments-crust boundary (Figure 9). For this first layer of the south intermediate velocity model (sediments section), the 2D starting velocity model was generated from a 1D reference velocity model that best fits the bathymetry-corrected traveltimes of Pg arrivals for the considered data set (OBS 31-38 + negative offset of OBS 39-43). The initial sediments-crust reflector was set to be horizontal at 7 km depth. Only the sediments refracted and reflected phases were included in the modelling.

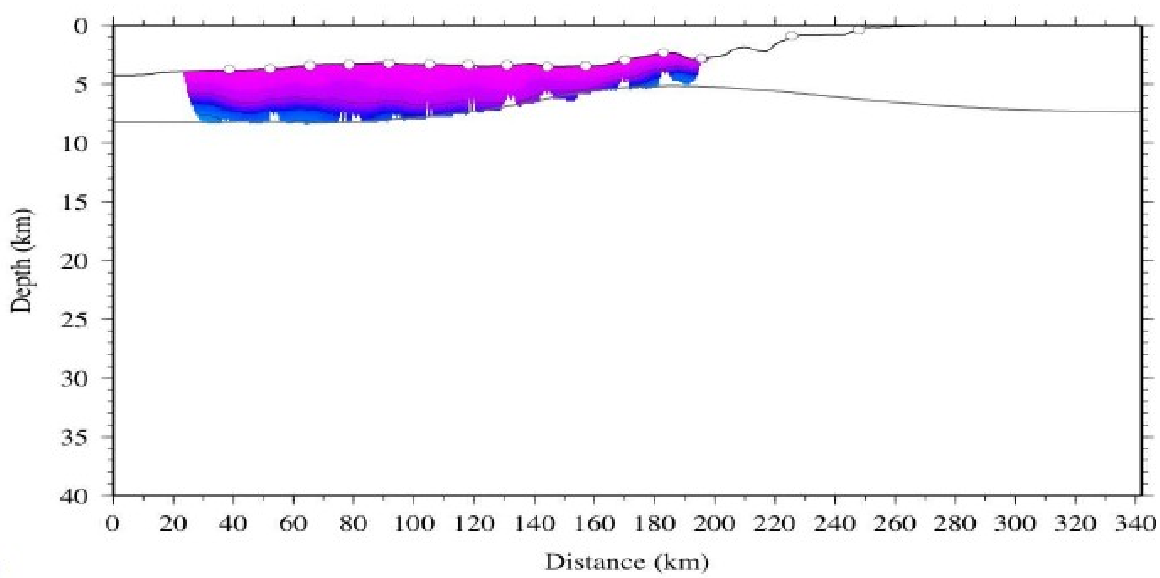

Figure 9.- Seismic velocity model of the sedimentary layer obtained by joint inversion of Ps and PsP phases along profile P2

The sedimentary section was then held weighted for the following inversion procedure, the latter being the inversion of the P-wave velocity structure for the crust using Pg and PmP arrivals in order to derive the crustal velocity field and Moho depth (Figure 10). To weight the structures obtained for the sediments unit inversion, a 2D velocity damping field with either large or low weighting factors depending on the zone to retain or invert in the considered inversion is defined.

For the second layer of the south intermediate velocity model (crustal section), the 2D starting velocity model was built as follows: (i) the previously determined sedimentary section was weighted by using spatial damping (Korenaga et al., 2000), and (ii) the crustal section underneath was represented by an arbitrary 1D velocity model varying from 5 km/s at ~8 km depth to 7 km/s at ~15 km depth with a constant vertical velocity gradient. The initial Moho reflector was set to be horizontal at 16 km depth. In this modelling step, we included sediments and crustal refracted phases (Pg) to their maximum offset, and the Moho was defined using the PmP phase simultaneously in the tomographic inversion. The final south intermediate 2D velocity model is shown after 8 iterations of the inversion procedure.

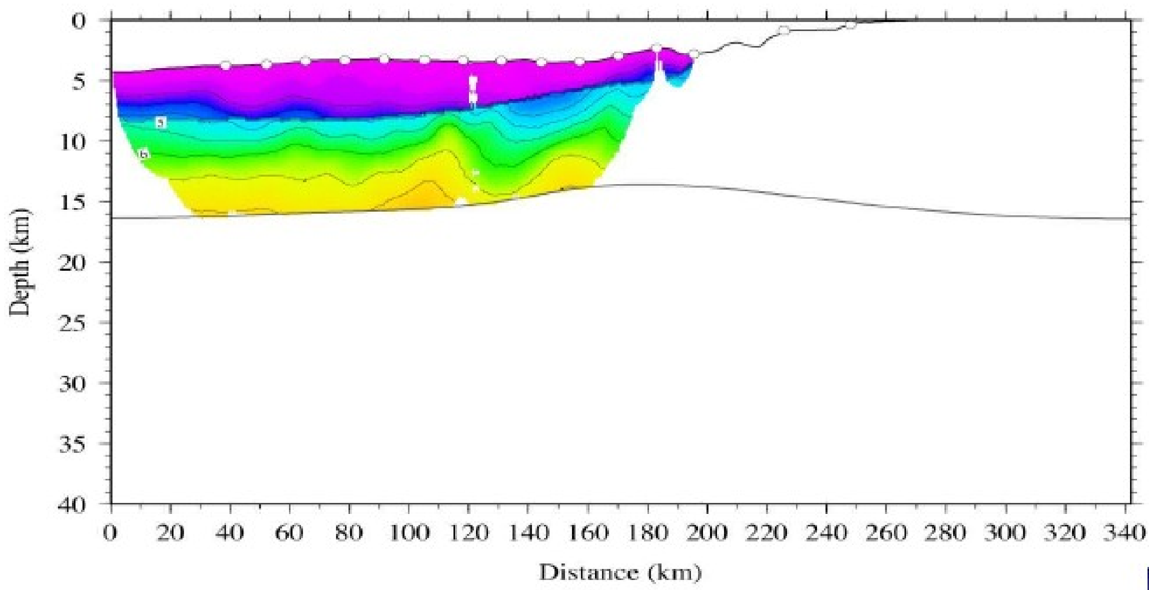

Figure 10.- Seismic velocity model of the sediments and oceanic crust obtained by joint inversion of Ps, Pg and PmP phases along profile P2

The intermediate velocity model for the north part of the profile (north intermediate velocity model) was constructed using one layer only (sediments + crust) as no clear sediment refracted Ps phases could be identified on the record sections in this area. Here, sediments and crust were inverted together using Pg and PmP phases to model the corresponding velocity field and Moho geometry (Figure 11).

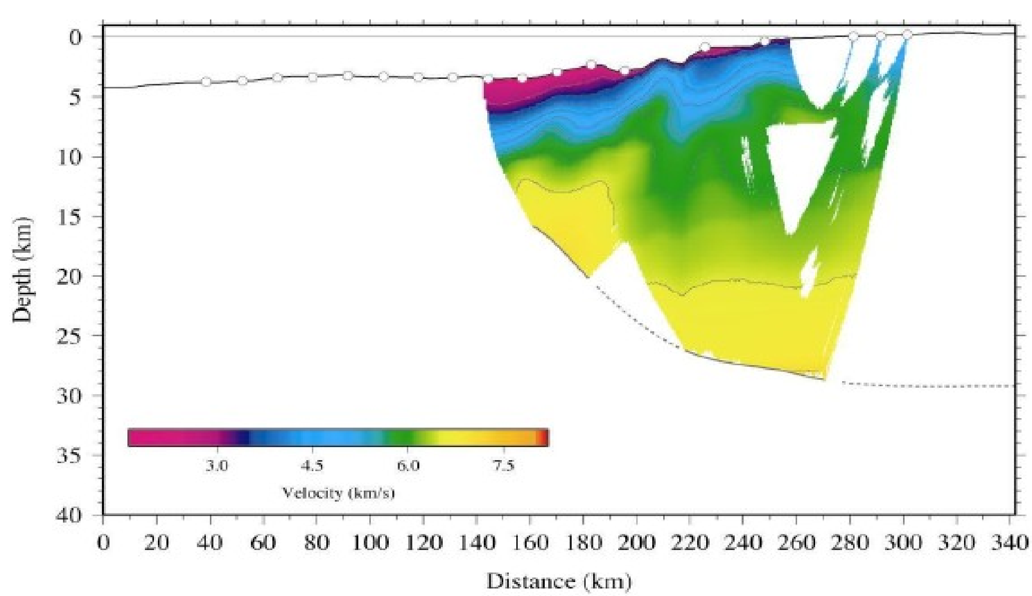

Figure 11.- Seismic velocity model of the sediments and crust at the ocean-continent transition zone obtained by joint inversion of Ps, Pg and PmP phases along profile P2

For the north intermediate velocity model, the 2D starting velocity model was generated from two 1D reference velocity models, which correspond to: (i) for the offshore part, the 1D log that best fits Pg arrivals from the OBS data located in the Algarve basin (positive offset of OBS 39-43 + OBS 44-45 (figure 3a, right)), and (ii) for the on-land part, a 1D log derived from a seismic refraction study done in this area (Palomeras et al., 2008). At the sea-land transition, the seismic velocities of the reference model were calculated by linerarly interpolating the two 1D velocity logs (figure 3a, right). The initial Moho reflector was set to be horizontal at 28 km depth. In this modelling step, we included sediments and crustal refracted phases (Pg) to their maximum offset, and the Moho was defined using the PmP phase simultaneously in the tomographic inversion. The final north intermediate 2D velocity model is shown after 7 iterations of the inversion procedure.

In the last step, the two intermediate models obtained were merged together and a new inversion was performed: the whole Ps, Pg, PmP and Pn arrivals were inverted for the final and complete velocity field of the sediments, crust and mantle along the entire profile (Figure 12). As Pn phases were little numerous compared with the other arrivals picked, the mantle velocity structure was inverted at this stage only. And as the Moho geometry was ready well defined from the intermediate velocity models, we chose to apply a high smoothing in depth during this last inversion.The reference velocity model for the final inversion step was built as follows: (i) the previously determined sedimentary and crustal structures for the south and north parts of the profile were merged together and weighted by using spatial damping, and (ii) the mantle section underneath was represented by an arbitrary 1D velocity model varying from 7.5 km/s at ~16 km depth to 8.5 km/s at ~35 km depth with a constant vertical velocity gradient. The reference Moho was also constructed by merging the final Moho previously obtained for the south and north intermediate models. All Ps, Pg, Pmp and Pn arrivals form the entire data set were included in this last inversion step. The final 2D velocity model is shown after 7 iterations of the inversion procedure. Sediments and crustal velocity structures obtained are almost identical to the one resulting from the intermediate steps.

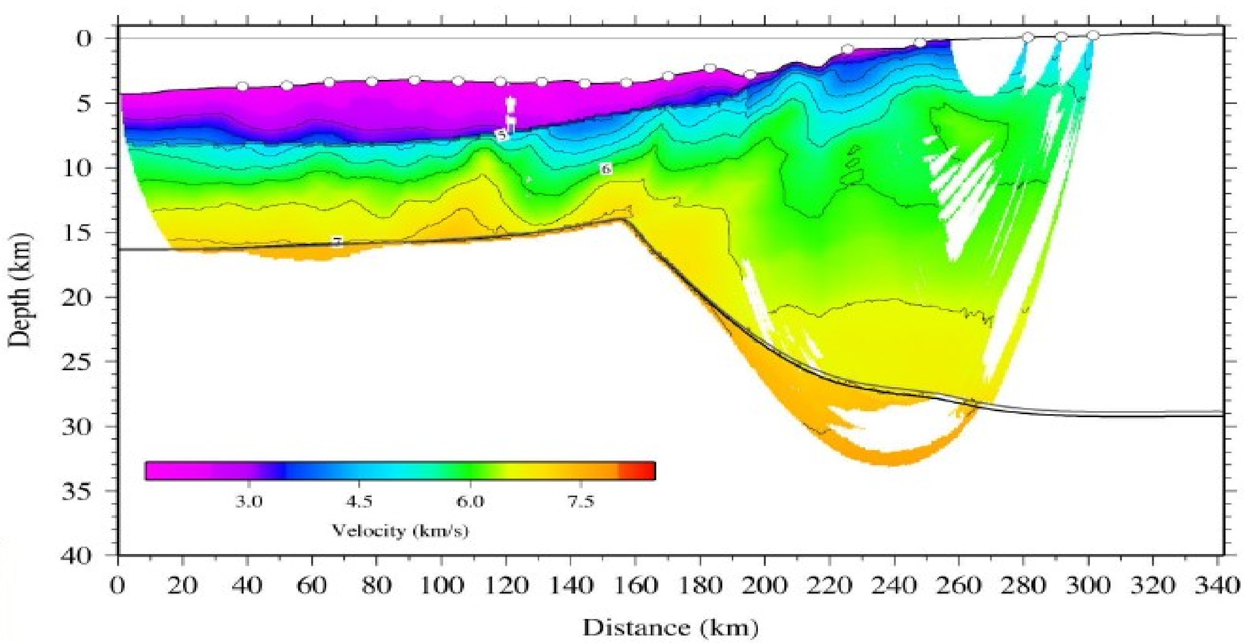

Figure 12.-Full seismic velocity model of the sediments, crust and upper mantle obtained by joint inversion of Ps, Pg, PmP and Pn phases along profile P2

The decrease of the root mean square (RMS) value from the first to the last iteration for both intermediate and merged models is significant, from 431 to 65 miliseconds. This rms reduction indicates a good convergence of the inversion procedure at each step of this hybrid approach of layer-stripping tomography. Examples of picked and calculated travel times for intermediate models and corresponding ray-tracing are shown in figures 13 and 14.

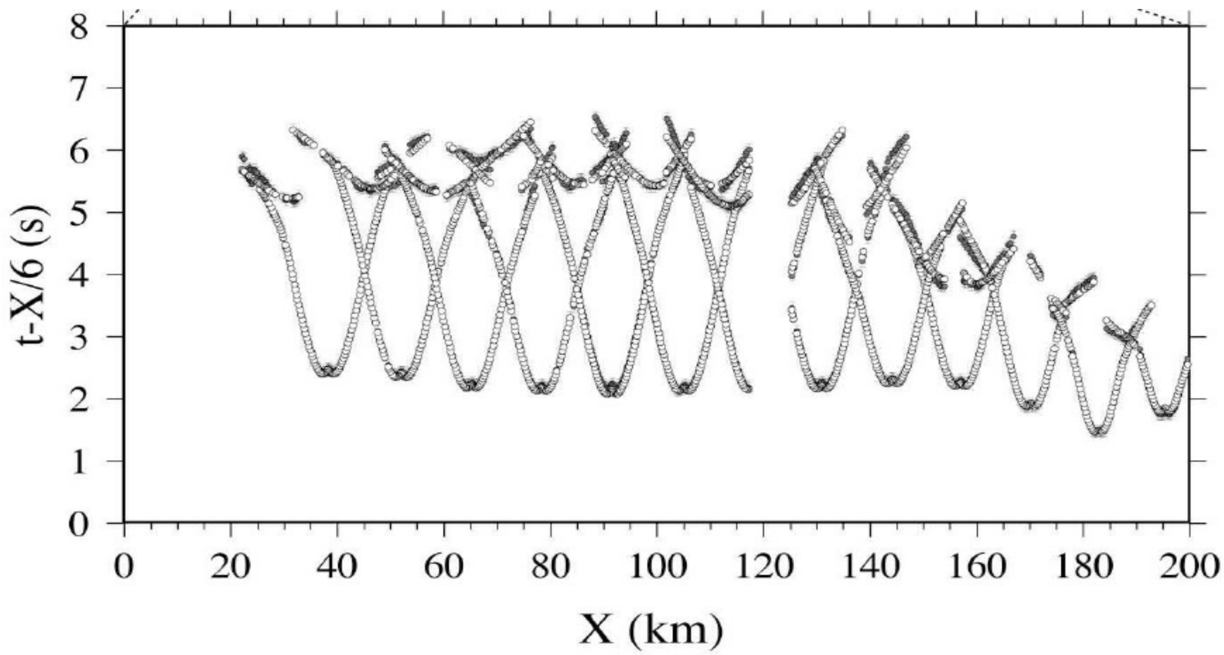

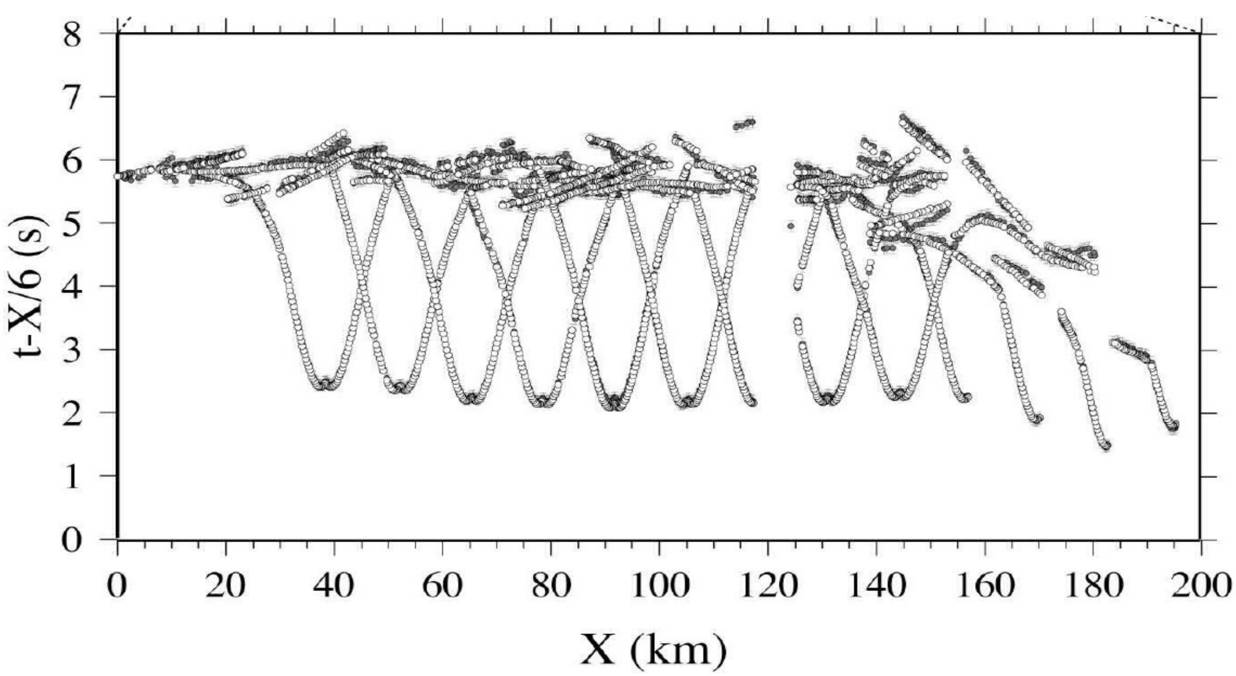

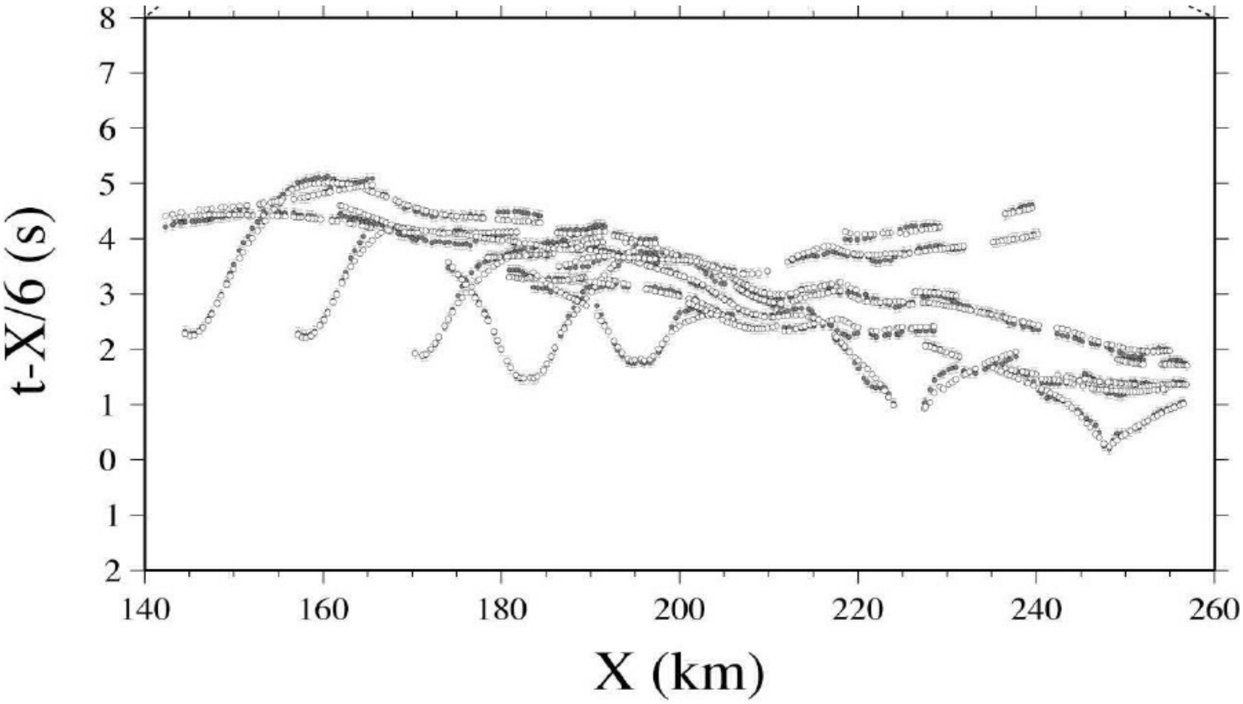

Figure 13.- Observed travel times for Ps and PsP phases (top) and Ps, Pg, and PmP phases (mid) (solid circles with error bars) and calculated traveltimes (white circles), at all OBS along P2, using the velocity model shown in figure 12. The bottom panel is the same as the mid one but for the northernmost OBS and landstations (ocean-continent transition)

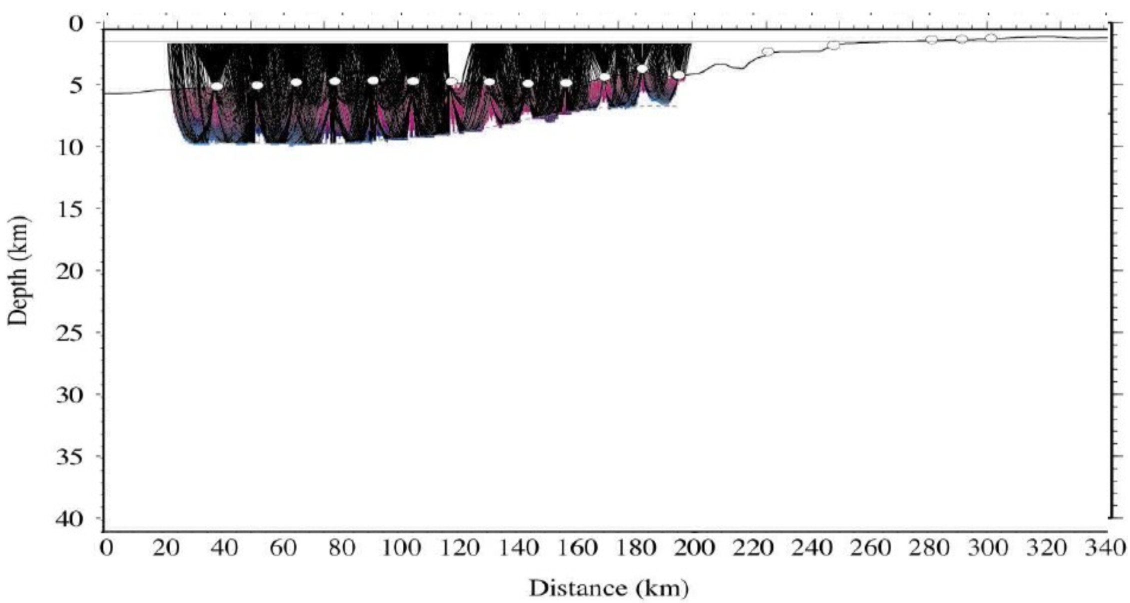

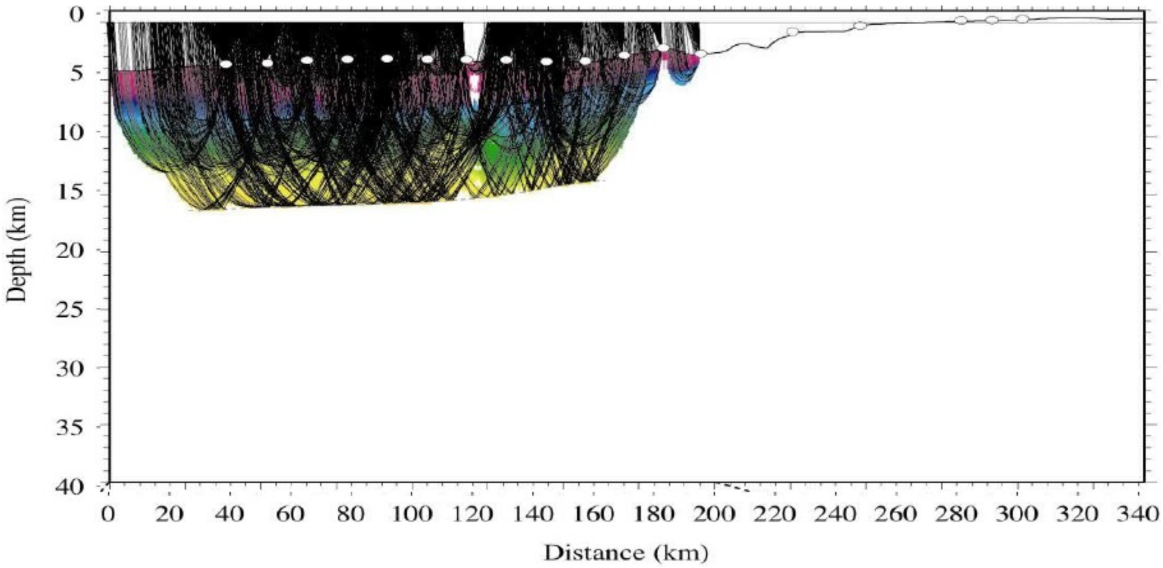

Figure 14.- Ray-tracing of seismic phases used to construct the models shown in Figures 9 (up) and 10 (botom).

5.3. Profile P1

The intermediate velocity model for the TAP, GB and HAP and SAP in the northern half of the profile was constructed using two layers: (1) sediments and (2) basement. The sediment refracted Ps and reflected PsP phases were used to invert for the velocities and thickness of the thick sedimentary cover,and hence the geometry of the sediments-basement boundary. (Figure 15). For this first layer of the south intermediate velocity model (sediments section), the 2D starting velocity model was generated from a 1D reference velocity model that best fits the bathymetry-corrected traveltimes of Pg arrivals for the considered data set (OBS 1-30). The initial sediments-crust reflector was set to be horizontal at 7 km depth. Only the sediments refracted and reflected phases were included in the modelling.

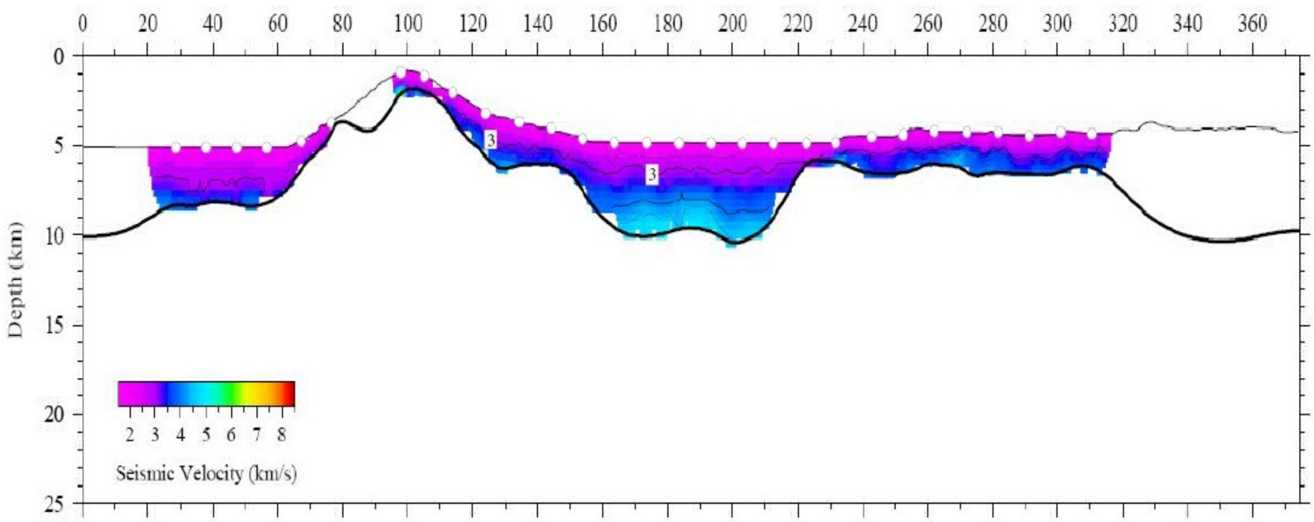

Figure 15.- Seismic velocity model of the sedimentary layer obtained by joint inversion of Ps and PsP phases along profile P1

The sedimentary section was then held weighted for the following inversion procedure, the latter being the inversion of the P-wave velocity structure for the crust using Pg and PmP arrivals in order to derive the crustal velocity field and Moho depth. Crustal phases were only identified in the southern part of the profile P1, this is at the SAP. The model obtained by joint Ps, Pg and PmP inversion in this sector of P1 is shown in Figure 16. To weight the structures obtained for the sediments unit inversion, a 2D velocity damping field with either large or low weighting factors depending on the zone to retain or invert in the considered inversion was defined as in the case of P2.

For the second layer of the SAP (crustal section), the 2D starting velocity model was built as follows: (i) the previously determined sedimentary section was weighted by using spatial damping, and (ii) the crustal section underneath was represented by a 1D velocity model with a velocity gradient varying from 5 km/s at ~8 km depth to 7 km/s at ~15 km depth. As in P2, the initial Moho reflector was set to be horizontal at 16 km depth. In this modelling step, we included sediments and crustal refracted phases (Pg) to their maximum offset, and the Moho was defined using the PmP phase simultaneously in the tomographic inversion. The final south intermediate 2D velocity model is shown after 9 iterations of the inversion procedure.

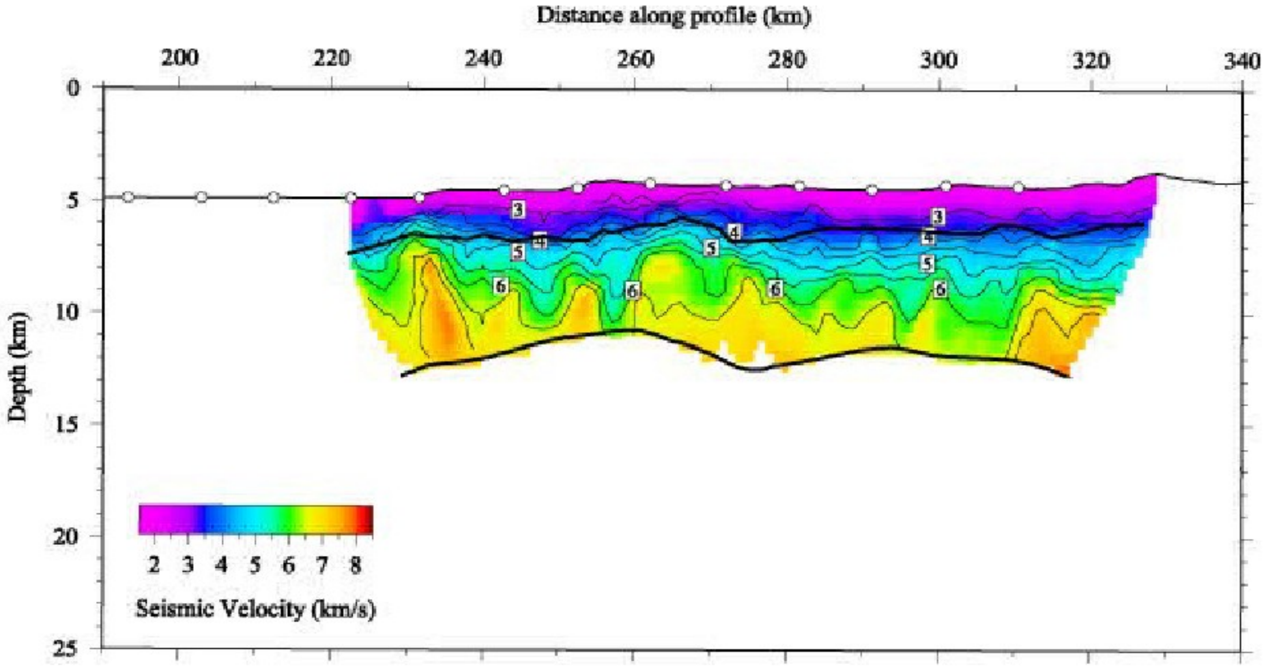

Figure 16.- Seismic velocity model of the sediments and oceanic crust obtained by joint inversion of Ps, Pg and PmP phases along the southernmost part of profile P1 (i.e., the Seine Abyssal Plain).

In the last step, the two intermediate models obtained were merged together and a new inversion was performed: the whole Ps, Pg, PmP and Pn arrivals were inverted for the final and complete velocity field of the sediments, crust and mantle along the entire profile (Figure 17). Most of the phases identified in the record sections along P1 were therefore identified as Pn, this is mantle refractions. As stated above, the only place were crust—mantle boundary reflections were identified is SAP, which means that in the rest the basement in probably not crust but mantle (Pn phases). The Moho geometry was ready well defined from the intermediate velocity models, so we choose to apply a high smoothing in depth during this last inversion.The reference velocity model for the final inversion step was built as follows: (i) the previously determined sedimentary and crustal structures for the south and north parts of the profile were merged together and weighted by using spatial damping, and (ii) the mantle section underneath was represented by an arbitrary 1D velocity model varying from 7.5 km/s at ~16 km depth to 8.3 km/s at ~35 km depth with a constant vertical velocity gradient. The reference Moho was also constructed by merging the final Moho previously obtained for the south and north intermediate models. All Ps, Pg, Pmp and Pn arrivals form the entire data set were included in this last inversion step. The final 2D velocity model is shown after 8 iterations of the inversion procedure.

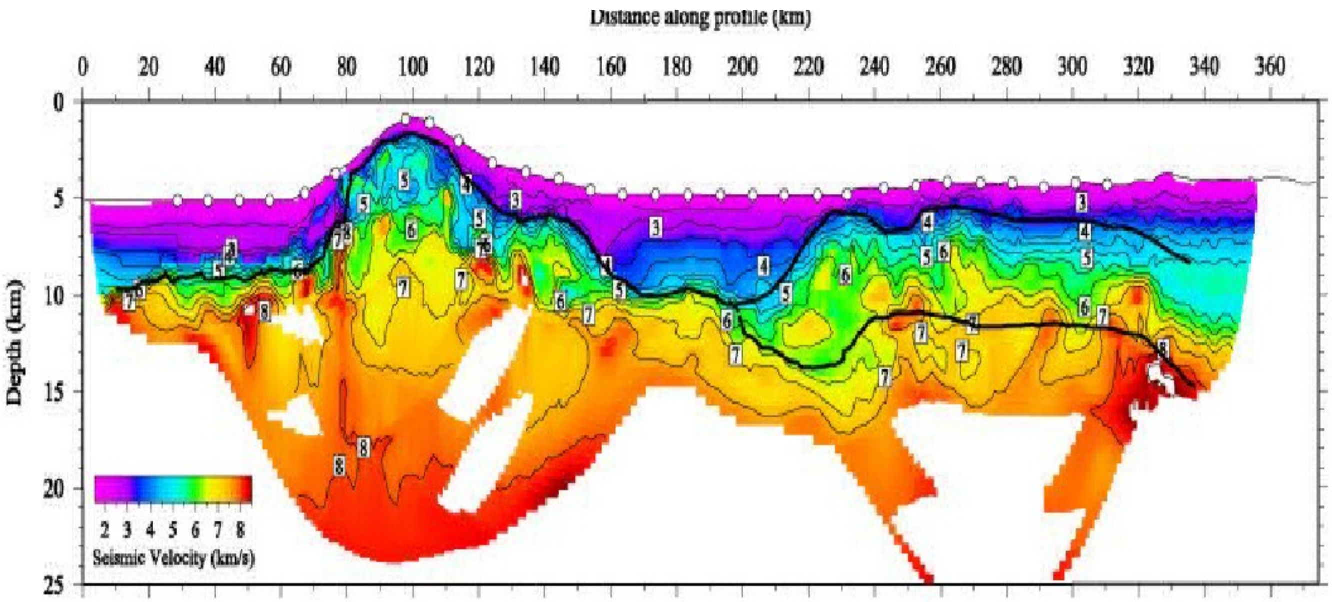

Figure 17.- Full seismic velocity model of the sediments, crust and upper mantle obtained by joint inversion of Ps, Pg, PmP and Pn phases along profile P1

The decrease of the root mean square (RMS) value from the first to the last iteration for both intermediate and merged models is significant, from 520 to 82 miliseconds. This rms reduction indicates a good convergence of the inversion procedure at each step of this hybrid approach of layer-stripping tomography. However, the inversion, specially for the upper mantle should be improved, to have a smoother velocity model, since most of the short-wavelength variations present in the model are most likely due to spurious phases identified as real in the record sections. Examples of picked and calculated travel times for intermediate models and corresponding ray-tracing are shown in figures 18 and 19.

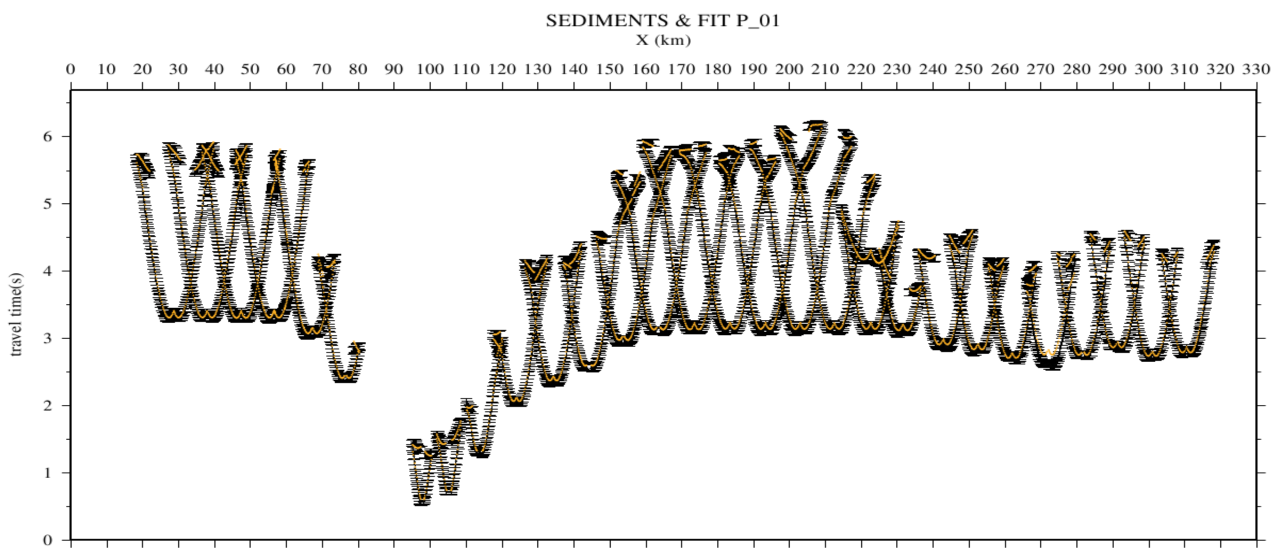

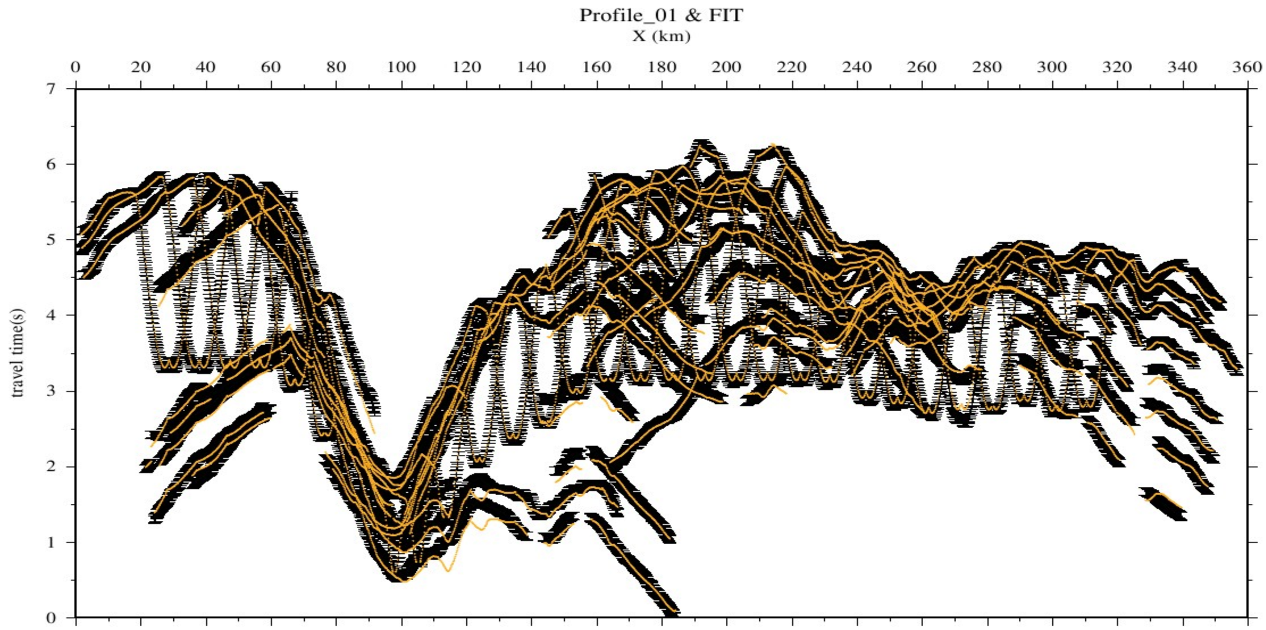

Figure 18.- Observed travel times for Ps and PsP phases (top) and Ps, Pg, and Pn phases (bottom) (solid circles with error bars) and calculated traveltimes (white circles), at all OBS and landstations along P1, using the velocity model shown in figure 17.

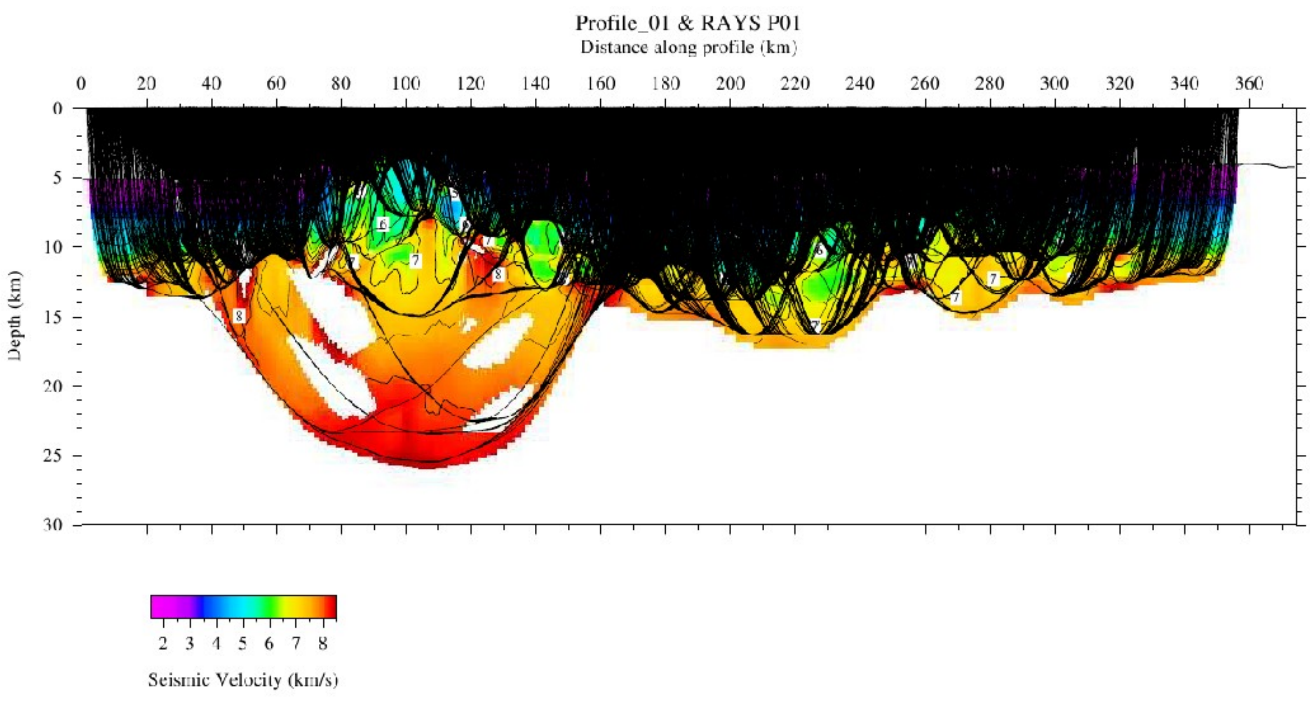

Figure 19.- Ray-tracing of seismic phases used to construct the models shown in figure 17.

The derivative weight sum (DWS), which is the column sum vector of the velocity kernel

(Toomey and Foulger, 1989) and provides information on the ray density and thus the linear sensitivity of the inversion, is shown for the final velocity model in Figure 20.

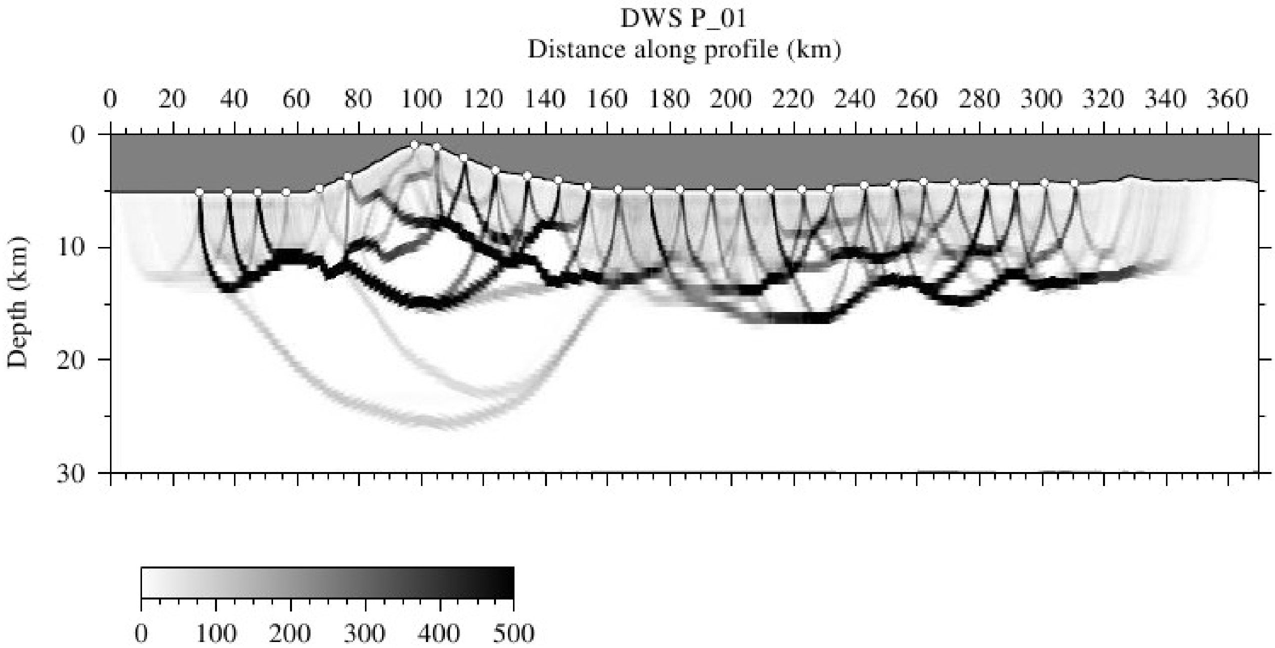

Figure 20.- Derivative weight sum corresponding to the velocity model displayed in figure 17

6. Uncertainty analysis and sensitivity test

6.1. Uncertainty analysis of model parameters

Statistical uncertainty analysis is becoming a common pool to evaluate how reliable the inverted velocity and reflector geometry actually are. Monte Carlo-like techniques as those originally proposed by Tarantola (1987), have been applied to wide-angle seismic data modelling in order to evaluate the level of dependency of the final model on the starting model, the validity of the methodological approximations made (e.g. linearization), the limitations derived of the experiment setup, as well as the influence of picking errors. We have therefore conducted a statistical uncertainty analysis following the same approach for each step of the modelling process: (1) generation of a set of 100 2D starting Monte Carlo ensembles was generated by randomly perturbing velocities (±0.35 km/s) of the reference models. Associated noisy data set was constructed by adding random common phase errors (±50 ms) and common receiver errors (±50 ms) to the initial reference data set. (2) the iterative inversion of each of the 100 perturbed velocity models and noisy data set was then performed. The mean deviation of all realizations of such an ensemble is a statistical measure of the model parameters uncertainties (Tarantola, 1987). The same inversion procedure has been followed and depicted in previous works in other areas (e.g., Sallarès et al., 2005; Gailler et al., 2007, 2009). Results from our calculations for the sediments and the crust are shown in figures 21, 22 and 23. As stated in the previous section, at this stage we have only made the uncertainty analysis of profile P2. The same approach will be applied to P1 once the modelling is finished.

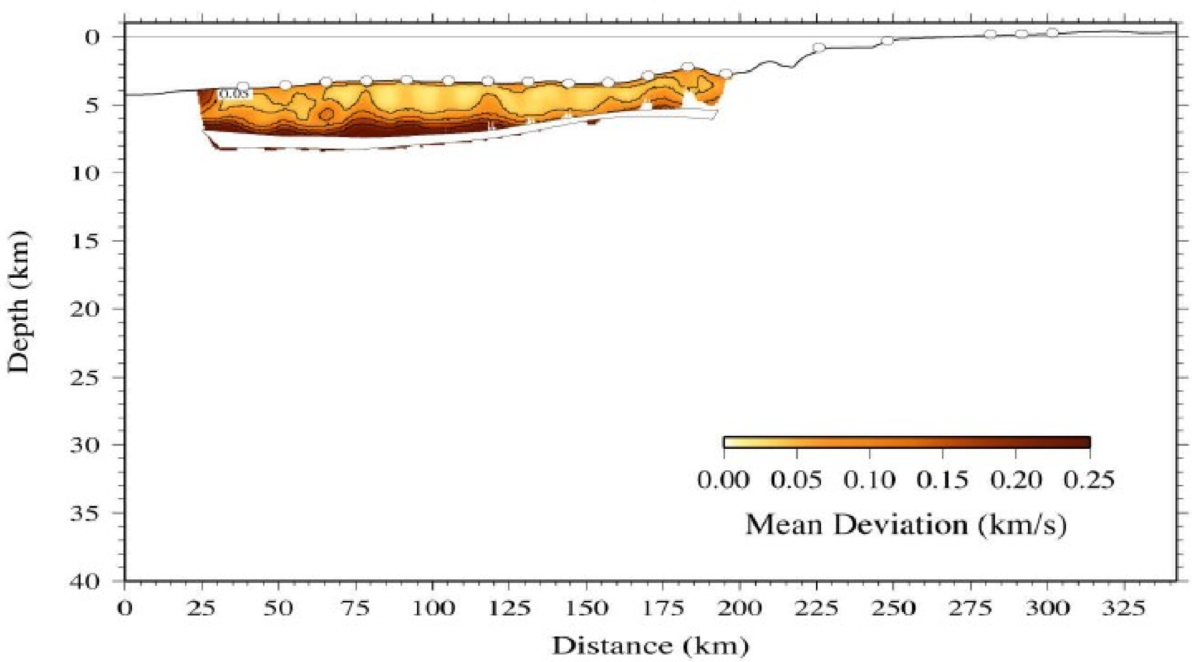

Figure 21.- Uncertainty of sediments velocity and the geometry of the top of the basement corresponding to model shown in figure 9.

Uncertainties in the accretionnary wedge sediments section are low (~0.1 km/s), except close to the sediments-crust reflector (~0.20 km/s), due to a trade-off between Pg refracted and Pr reflected phases sampling this area (figure 21). Uncertainties below in the crust are also low (~0.1 km/s), confirming that we can be confident in the velocity values obtained for the south part of the model (up to 160 km distance). The geometry and depth of the sediments-crust and crust-mantle boundaries in this area are also accurately determined, with ~0.5 km depth uncertainty or even less (figure 22).

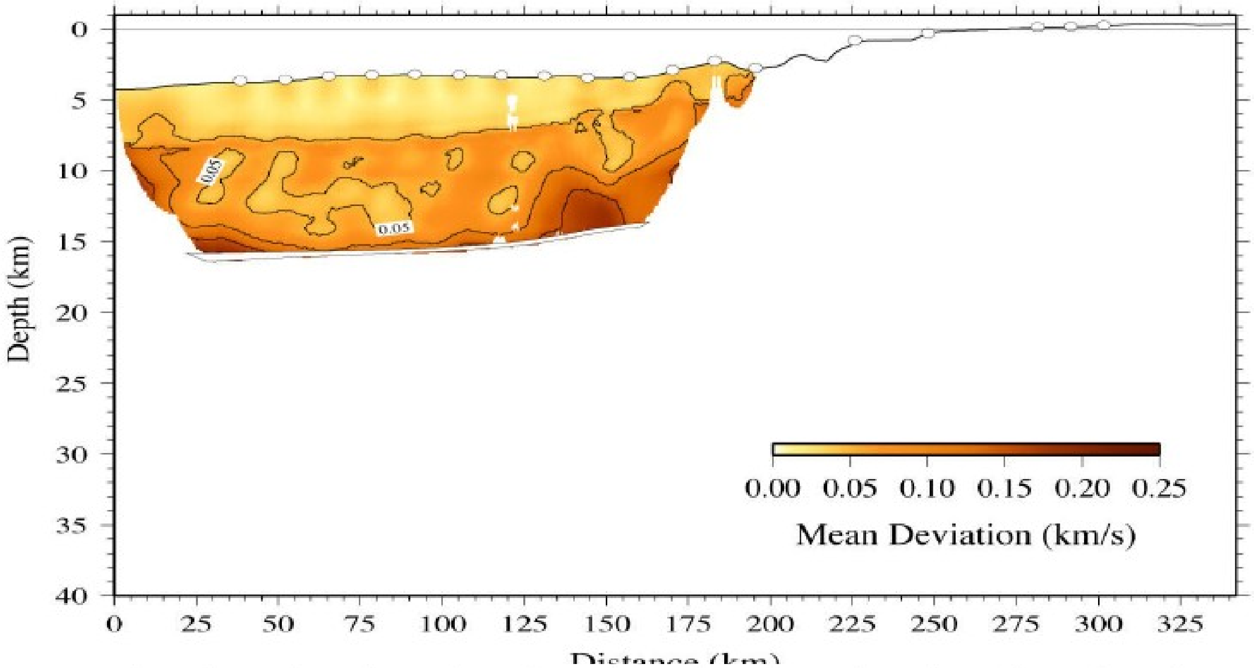

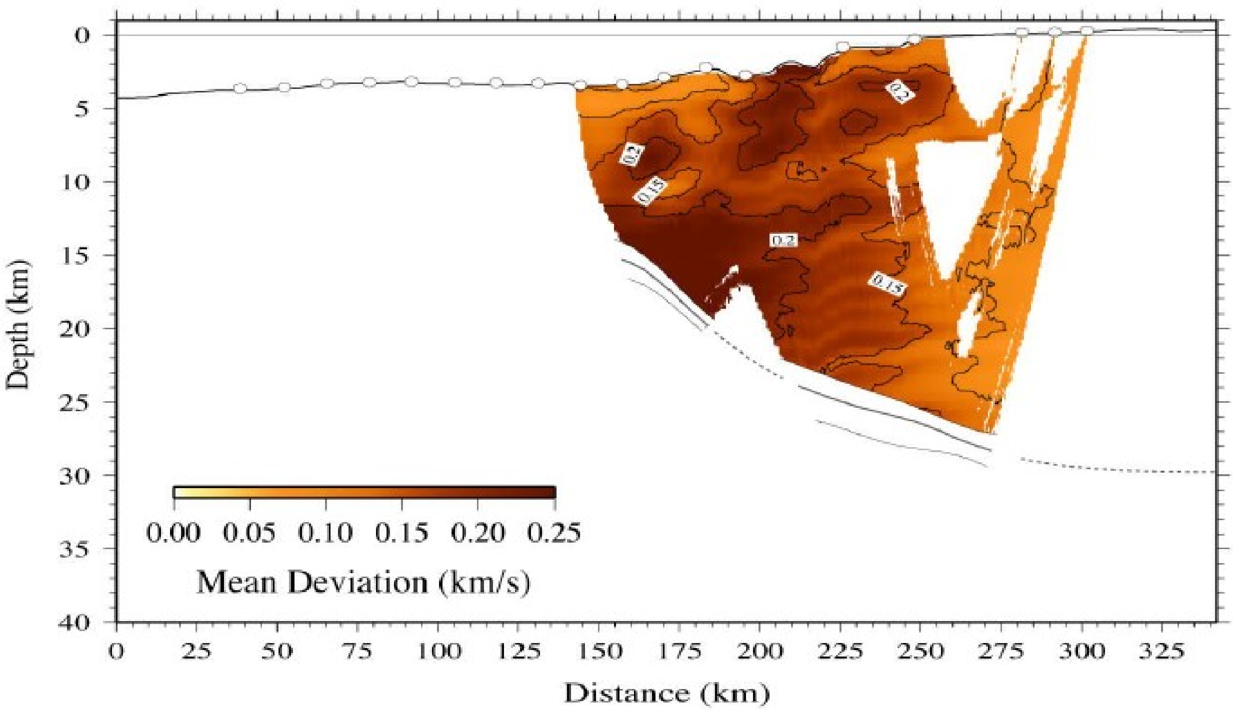

Fi... ho
co...

Th... ce)
sh... 3).
Ur... city
va... ay
co... nP
arı... es
of ... ure
23...

Th... a
lac... a
re... es
tha...

Figure 23.- Uncertainty of crustal velocity and the geometry of the Moho at the continent-ocean transition corresponding to the model shown in figure 11.

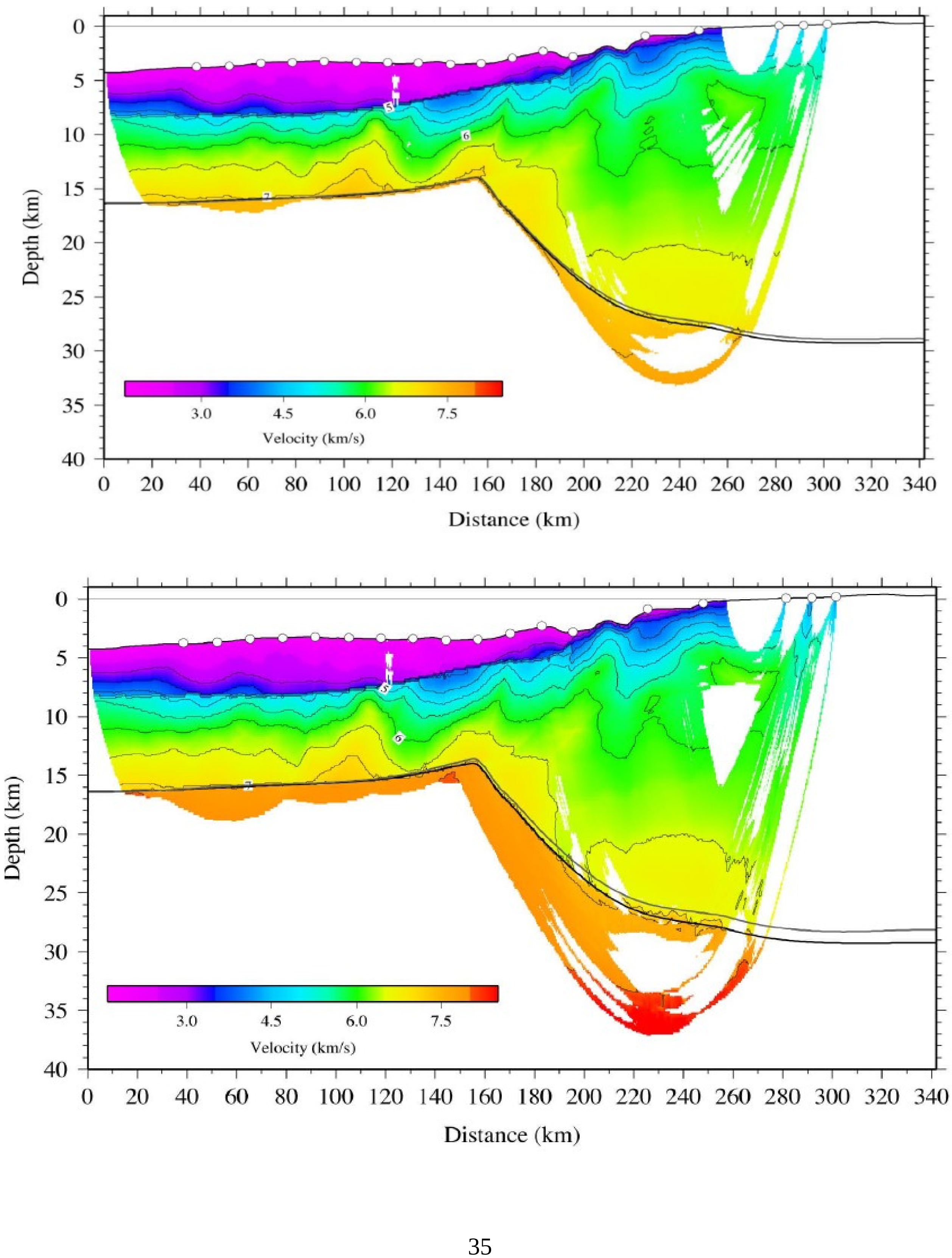

Figure 24.- Sensitivity test made for mantle velocities. The model in the upper panel has been obtained wit a initial mantle velocity of 7.0 km/s, and the bottom panel with a mantle velocity of 8.0 km/s.

For the complete model (Figure 11) an additional test has been done to check how well resolved the mantle velocities actually are. For this the velocity of the reference model was changed between 7.0 km/s and 8.0 km/s, keeping the rest of the model fixed. Figure 24 show the results obtained with these two initial models after 6 iterations. The results indicate that the remarkably low mantle velocities obtained are a real, robust feature and not a modeling artifact.

7. Results and conclusions

The region offshore the SW Iberian margin hosts the present-day NW-SE plate convergence between the European and African Plates at a rate of 4.5 mm/yr, fact that causes continuous seismic activity of moderate magnitude in the area. In autumn 2008 a Spanish-French team carried out a refraction and wide-angle reflection seismic survey in the area (NEAREST-SEIS cruise), in the framework of the EU, FP6-funded NEAREST project. During the survey two long seismic profiles were acquired using a pool of 36 Ocean Bottom Seismometers (OBS), with the objectives of providing information about the geometry of the crust-mantle boundary and the physical properties of the crust, revealing the deep geometry of the main fault interfaces, and identifying the nature of the basement and the limits of the different geological provinces in the region.

The results obtained to date are almost definitive along P2, where the full sequenbce of data acquisition, processing, seismic phase identification, picking and refinement, wide-angle data modelling and uncertainty analysis has been completed. In the case of P1, there is still work to be done specially concerning data picking refinement and uncertainty analysis.

In sections 7.1 and 7.2 we make a brief description of the results obtained along those two profiles. The interpretation made is preliminary, specially in the case of P1, and could vary depending on the final modelling. In the case of P2 the model obtained is more reliable and the interpretation made is thus more robust.

7.1. Seismic structure along P1

A total of 30 OBS were deployed along profile P1, which is 356 km long and extends from the Tagus abyssal plain (TAP), crossing the Gorringe bank (GB), the Horseshoe abyssal plain (HAP) and the Coral Patch Ridge (CPR), and the thrust-and-fold belt of the Seine abyssal plain (SAP). The acquired data were modelled by joint refraction and reflection traveltime inversion, following a layer-stripping strategy. The inverted model show four well-differentiated domains in terms of its seismic structure: In the TAP a 3-4 km-thick, low velocity sedimentary layer that covers the basement, which shows a strong velocity gradient reaching remarkably high velocity (>7.5 km/s) at very shallow level (<2 km below top of the basement). The velocity structure of the Gorringe ban is similar to the TAP, showing a finer layer of sediments covering a high velocity basement that likely correspond to mantle instead of crust. In the HAP the sedimentary cover is thicker, showing an upper unit with low velocity corresponding to the Horseshoe gravitational unit, on top of a higher velocity lower unit, which may represent the highly consolidated Mesozoic sedimentary sequence. The thickness of the two units together exceeds 5 km in most of the HAP. The basement shows the same velocity distribution as in TAP and GB, suggesting a common nature and origin. According to its seismic structure, and considering that there is no evidence for the presence of a basal reflector (e.g. Moho) in the record sections, we interpret this basement as highly serpentinized, exhumed mantle. In contrast, the CPR and SAP show evidences for the presence of a well-developed, 6-7 km-thick oceanic crust, underlying the 2-3 km-thick, moderate velocity, Mesozoic sedimentary sequence.

7.1 Seismic structure along P2

Profile P2 is 256 km long, and trends S-N extending from the easternmost Seine abyssal plain beyond the NW Moroccan margin, crossing the Gulf of Cadiz imbricated wedge and the Portimao bank ending at the Iberian margin shelf. 15 OBS and 7 land-stations were deployed along this profile, and the recorded data were modelled following the same approach and strategy as for P1. The inverted model shows two main domains: In the southern half, there is a 3-4 km-thick cover of low velocity sediments, which represents the western edge of the sedimentary wedge that covers the internal Gulf of Cadiz, overlying a 7-8 km-thick oceanic crust. According to recent tectonic reconstructions, this crustal segment should have been emplaced there during the early phase of continental spreading between Iberia and Africa, in the context of Mesozoic Atlantic spreading. The northern part of P2 displays a relatively sharp ocean-continent transition zone concentrated in a ~50 km-wide band, that ends with the ~30 km-thick continental crust of the SW Iberian shelf.

8. References

Argus, D.F., Gordon, R.G., Demets, C., Stein, S., 1989. Closure of the Africa-Eurasia-North America plate motion circuit and tectonics of the Gloria fault, J. Geophys. Res. 94, 5585-5602.

Avedik, F., Renard, V., Allenou, J.P., and Morvan, B. 1993. Single bubble airgun array for deep exploration. *Geophysics* **38**, pp. 366–382.

Baptista, M.A., Heitor, S., Miranda, J.M., Miranda P.M.A., and Mendes Victor, L., 1998a. The 1755 Lisbon; Evaluation of the tsunami parameters, J. Geodynamics 25, 143-157.

Baptista, M.A., Miranda P.M.A., Miranda, J.M., and Mendes Victor, L., 1998b. Constraints on the source of the 1755 Lisbon tsunami inferred from numerical modelling of historical data on the source of the 1755 Lisbon tsunami. J. Geodynamics 25: 159-174.

Baptista, M.A., Miranda P.M.A., Chierici, F., and Zitellini, N., 2003. New study of the 1755 earthquake source based on multi-channel seismic survey data and tsunami modeling. Natural Hazards and Earth Science Systems 3: 333-340.

Barkan, R., ten Brink and Lin, J. 2009. Far field tsunami simulations of the 1755 Lisbon earthquake: Implications for tsunami hazard to the U.S. East Coast and the Caribbean, *Mar. Geol.* **264**, pp. 109–122.

Bokelmann, G., Maufroy, E., 2007, Mantle structure under Gibraltar constrained by seismic waveform complexity, Geophys. Res. Let., 34, L22305, doi:10.1029/2007GL030964

Buforn, E., Udias, A., and Colombas, M.A., 1988. Seismicity, source mechanisms and tectonics of the Azores-Gibraltar plate boundary, Tectonophysics, 152, 89-118.

Buforn, E., Sanz de Galdeano, C., and Udias, A., 1995. Seismotectonics of the Ibero-Maghrebian region, Tectonophysics, 248, 247-261.

Buontempo, L., Bokelman, G.H.R., Barruol, G., Morales, J., 2008. Seismic anisotropy beneath southern Iberia from SKS splitting. Earth Planet. Sci. Lett., 273, 237-250.

Contrucci, I., Klingelhoefer, F., Perrot, J., Bartolome, R., Gutscher, M.-A., Sahabi, M., Malod, J., and Rehault, J.-P., 2004. The crustal structure of the NW-Moroccan continental margin from wide-angle and reflection seismic data. Geophys. J. Int., (in press).

DeMets, C., R.G. Gordon, D.F. Argus, S. Stein, (1990). Current plate motions. Geophys. J. Int. 28, 2121-2124.

DeMets, C., Gordon, R.G., Argus, D.F., Stein, S. 1994. Effect of recent revisions to the geomagnetic reversal time scale on estimates of current plate motions, *Geophys. Res. Lett. 21* , 2191-2194.

Duggen, S., Hoernle, K., van den Bogaard, P., Harris, C., 2004. Magmatic evolution of the Alboran Region: The role of subduction in forming the western Mediterranean and causing the Messinian Salinity Crisis. Earth Planet. Sci. Lett. 218, 91-108.

Gailler, A., Charvis, P., Flueh, E., 2007, Segmentation of the Nazca and South American plates along the Ecuador subduction zone from wide angle seismic profiles, Earth Planet. Sci. Lett., 260 (34),444-464.

Gailler, A., Klingelhoefer, F., Olivet, J.L., Aslanian, D., and Sardinia-group. 2009. Crustal structure of a young margin pair: new results across the Liguro–Provencal Basin from wide-angle seismic tomography, *Earth Planet. Sci. Lett.* **236**, pp. 333–345.

Gracia, E., Danobeitia, J.J., Verges, J., Bartolome, R., 2003a. Crustal architecture and tectonic evolution of the Gulf of Cadiz (SW Iberian margin) at the convergence of the Eurasian and African plates. Tectonics 22, n.4, 1033, doi;10.1029/2001TC901045.

Gracia, E., Danobeitia, J.J., Verges, J., PARSIFAL Team, 2003b. Mapping active faults offshore Portugal (36°N-38°N): Implications for seismic hazard assessment along the southwest Iberian margin. Geology 31, 83-86.

Grevemeyer, I., Kaul, N., and Kopf, A., 2008. Heat flow anomalies in the Gulf of Cadiz and off Cape San Vicente, Portugal. Marine and Petroleum Geology, doi:10.1016/j.marpetgeo. 2008.08.006.

Gutscher, M.-A., Malod, J., Rehault, J.-P., Contrucci, I., Klingelhoefer, F., Mendes-Victor, L., Spakman, W., 2002. Evidence for active subduction beneath Gibraltar. Geology 30, 1071-1074.

Gutscher, M.-A., 2004. What caused the Great Lisbon Earthquake?, Science, v. 305, p. 1247-1248.

Gutscher, M.-A., Baptista, M.A., Miranda, J.M., 2006. The Gibraltar Arc seismogenic zone (part 2): constraints on a shallow east dipping fault plane source for the 1755 Lisbon earthquake provided by tsunami modeling and seismic intensity. Tectonophysics, Sp. Vol. “Natural laboratories on seismogenic faults”, v. 427, p. 153-166, doi:10.1016/j.tecto. 2006.02.025.

Gutscher, M.-A., Dominguez, S., Westbrook, G., Gente, P., Babonneau, N., Mulder, T., Gonthier, E., Bartolome, R., Luis, J, Rosas, F., Terrinha, P., and the Delila and DelSis Scientific Teams. 2009a. Tectonic shortening and gravitational spreading in the Gulf of Cadiz accretionary wedge: observations from multi-beam bathymetry and seismic profiling. Journal of Marine and Petroleum Geology, Sp. Vol. on Submarine instabilities. doi: 10.1016/j.marpetgeo.2007.11.008.

Gutscher, M.-A., Dominguez, S., Westbrook, G.K., and Le Roy, P., 2009b. Deep structure, recent deformation and analog modeling of the Gulf of Cadiz accretionary wedge: implications for the 1755 Lisbon earthquake. Tectonophysics Sp. Vol., Proc. of the MAPG Meeting Marrakech Morocco (guest editor D. Frizon de Lamotte)., v. 475, p. 85-97, doi: 10.1016/j.tecto.2008.11.031.

Hensen, C., Nuzzo, M., Hornibrook, E.R.C., Pinheiro, L., Bock, B., Magalhaes, V.H. and Brückmann, W., 2007. Sources of mud volcano fluids in the Gulf of Cadiz - indications for hydrothermal input, Geochim. Cosmochim. Acta, v.71, 1232-1248 doi:10.1016/j.gca. 2006.11.022.

Hinz K. Hinz, H. Dostmann, J. Fritsch, The continental margin of Morocco : seismic sequences, structural elements and the geological development, in : U. Von Rad, K. Hinz, M. Sarntheim, E. Seibold (Eds.), Geology of the North West African Continental Margin, Springer - Verlag, Berlin Heidelberg NewYork, 1982, pp. 34-60.

Iribarren, L., Verges, J., Camurri, F., Fullea, J., Fernandez, M., 2007. The structure of the

Atlantic-Mediterranean transition zone from the Alboran Sea to the Horseshoe Abyssal Plain (Iberia – Africa plate boundary). Marine Geology, 243, 97-119. doi:10.1016/j.margeo.2007.05.011.

IOC, IHO and BODC, 2003. “Centenary edition of the GEBCO Digital Atlas“, published on CD-ROM on behalf of the Intergovernmental Oceanographic Commission and the International Hydrographic Organization as part of the General Bathymetric Chart of the Oceans; British Oceanographic Data Centre, Liverpool.

Johnston, A., 1996. Seismic moment assessment of earthquakes in stable continental regions – III. New Madrid, 1811-1812, Charleston 1886 and Lisbon 1755. Geophys. J. Int. 126, 314-344.

Korenaga, J., W. S. Holbrook, G. M. Kent, P. B. Kelemen, R. S. Detrick, H.-C. Larsen, J. R. Hopper, and T. Dahl-Jensen (2000), Crustal structure of the southeast Greenland margin from joint refraction and reflection seismic tomography, J. Geophys. Res., 105, 21,591–21,614.

Lonergan, L. and White, N., 1997. Origin of the Betic-Rif mountain belt. Tectonics 16, 504-522.

Martinez-Solares, J.M., Lopez A., and Mezcua, J., 1979. Isoseismal map of the 1755 Lisbon earthquake obtained from Spanish data. Tectonophysics 53, 301-313.

McClusky, S., Reilinger, R., Mahmoud, S., D.Ben Sari, D., and Tealeb, A., 2003. GPS constraints on Africa (Nubia) and Arabia Plate motions Geophysical Journal International, 155, 1, 126-138.

Nocquet, J.M., and Calais, E., 2004. Geodetic measurements of crustal deformation in the Western Mediterranean and Europe. Pure Appl. Geophys., 161, 661-681.

Olivet, J.-L., 1996. La cinématique de la Plaque Ibérique, Bull. Cent. Rech. Elf Explor. Prod., 20, 131-195.

Palomeras, I., Carbonell, R., Flecha, I., Simancas, J.F., Ayarza, P., Mata, D., Martínez Poyatos, D., Azor, A., Gonzalez Lodeiro, F. and Pérez Estaún, A. 2008 Constraints on the Lithosphere across the Variscan Orogen of SW Iberia from dense wide-angle seismic reflection data, *Journal of Geophysical Research* (2008) 10.1029/2007JB005564.

Pinheiro, L.M., Ivanov, M.K., Sautkin, A., Akhmanov, G., Magalhaes, V.H., Volkonskaya, A., Monteiro, J.H., Somoza, L., Gardner, J., Hamouni, N., Cunha, M.R., 2003. Mud volcanism in the Gulf of Cadiz: results from the TTR-10 cruise. Marine Geology 195, 131-151.

Pinheiro, L.M., et al. 2006. MV Seis: Tectonic control, deep crustal structure and fluid escape pathways in the Gulf of Cadiz Mud Volcano Field. EuroMargins Interim Report, ESF Project 01-LEC-EMA24F.

Roest, W. and Srivastava, S., 1991. Kinematics of the plate boundaries between Eurasia, Iberia, and Africa in the North Atlantic from the Late Cretaceous to the present, Geology, 19, 613–616

Rovere, M., Ranero C., Sartori, R., Torelli, L., and Zitellini, N. (2004). Seismic images and magnetic signature of the Late Jurassic to Early

Cretaceous Africa–Eurasia plate boundary off SW Iberia

, Geophys. J. Int., 158, 554–568.

Sahabi, M., Aslanian, D., and Olivet, J.-L., 2004. A new starting point for the history of the Central Atlantic, C.R.A.S. Paris, 336, 1041-1052.

Sallarès, V., P. Charvis, E. R. Flueh, J. Bialas, and SALIERI Working Group (2005), Seismic structure of Carnegie Ridge and the nature of the Galapagos hotspot, Geophys. J. Int., in press.

Somoza, L., Diaz-del-Rio, V., Leon, R., Ivanov, M., Fernandez-Puga, M.C., Gardner, J.M., Hernandez-Molina, F.J., Pinheiro, L.M., Rodero, J., Lobato, A., Maestro, A., Vazquez, J.T., Medialdea, T., Fernandez-Salas, L.M., 2003. Seabed morphology and hydrocarbon seepage in the Gulf of Cadiz mud volcano area: acoustic imagery, multibeam and ultrahigh resolution seismic data. Mar. Geol. 195, 153– 176.

Spakman, W. and Wortel, R., 2004 A tomographic view on Western Mediterranean Geodynamics. in The TRANSMED Atlas. The Mediterranean region from crust to mantle. Geological and Geophysical framework. 2004. Cavazza, W., Roure, F., Spakman, W., Stampfli, G., and Ziegler, P. (Eds.) Episodes, v. 27, p. 31-52.

Srivastava, S.P., Schouten, H., Roest, W.R., Klitgord, K.D., Kovacs, L.C., Verhoef, J. and Macnab, R., 1990. Iberian plate kinematics: a jumping plate boundary between Eurasia and Africa, Nature 344, 756-759.

Stampfli, G. M., Vavassis, I. De Bono, A. Rosselet, F. Matti, B. & Bellini, M. 2003. Remnants of the Palaeotethys oceanic suture-zone in the western Tethyan area. *In*: Cassinis, G. & Decandia, F. A. (eds) *Stratigraphic and Structural Evolution on the Late Carboniferous to Triassic Continental and Marine Successions in Tuscany (Italy): Regional Reports and General Correlation,* **2**, Bolletino della Società Geologica Italiana, Volume speciale, 1–24

Stich, D., Ammon, C.J., Morales, J., 2003. Moment-tensor solutions for small and moderate earthquakes in the Ibero-Maghreb region. J. Geophys. Res. 108, 2148.

Stich, D., Mancilla, F., Baumont, D. y Morales, J. (2005): Source analysis of the Mw 6.3 2004 Al Hoceima earthquake (Morocco) using regional apparent source time functions. Journal of Geophysical Research, 110: B06306, doi:10.1029/2004JB003366.

Stich, D., Serpelloni, E., Mancilla, F., Morales, J., 2006. Kinematics of the Iberia- Maghreb plate contact from seismic moment tensors and GPS observations. Tectonophysics 426, 295-317.

Stich, D., Mancilla F.d.L., Pondrelli S., Morales, J., 2007. Source analysis of the February 12th 2007, Mw 6.0 Horseshoe earthquake : Implications for the 1755 Lisbon earthquake. Geophys. Res. Lett., v. 34, L12308, doi :10.1029/2007GL030012.

Tahayt, A., Mourabit, T., Rigo, A., Feigl, K.L., Fadil, A., McClusky, S., Reilinger, R., Serroukh, M., Ouazzani-Touhami, A., Ben-Sari, D., and Vernant, P., 2008. Mouvements actuels des blocs tectoniques dans l’arc Bético-Rifain à partir des mesures GPS entre 1999 et 2005. Comptes Rendus Geoscience, 340, 400-413.

Tarantola, A. (1987), Inverse Problem Theory: Methods for Data Fitting and Model Parameter Estimation, 613 pp., Elsevier, New York.

Terrinha, P., Pinheiro, L.M., Henriet, J.-P., Matia, L., Ivanov, A.K., Monteiro, J.H., Akhmetzhanov, A., Volkonskaya, Cunha, M.R., Shaskin, P. and Rovere, M., 2002. Tsunamigenic-seismogenic structures, neotectonics, sedimentary processes and slope instability on the Southwest Portugese Margin. Marine Geology 195, 55-73.

Terrinha, P., Pinheiro, L.M., Henriet, J.-P., Matias, L., Ivanov, M.K., Monteiro, J.H., Akhmetzhanov, A., Volkonskaya, A., Cunha, T., Shaskin, P., Rovere, M., 2003. Tsunamigenic–seismogenic structures, neotectonics, sedimentary processes and slope instability on the southwest Portuguese Margin. Mar. Geol. 195, 55–73

Thiebot, E., and Gutscher, M.-A., 2006. The Gibraltar Arc seismogenic zone (part1): constraints on a shallow east dipping fault plane source for the 1755 Lisbon earthquake provided by seismic data, gravity and thermal modeling. Tectonophysics Sp. Vol. “Natural laboratories on seismogenic faults”, v. 427, p. 135-152, doi:10.1016/j.tecto.2006.02.024.

Toomey, D. R., and G. R. Foulger (1989), Tomographic inversion of local earthquake data from the Hengill-Grensdalur central volcano complex, Iceland, J. Geophys. Res., 94, 17,497– 17,510.

van Avendonk, H. J. A., A. J. Harding, and J. A. Orcutt (1998), A twodimensional tomographic study of the Clipperton transform fault, J. Geophys. Res., 103, 17,885– 17,899.

Verhoef, J., Collette, B. J., Danobeitia, J. J., Roeser, H. A., & Roest, W. R., 1991. Magnetic anomalies off West-Africa, Mar. Geophys. Res., 13, 81-103.

Vilanova, S.P., Nunes, C.F. and Foncesca, J.F.B.D., 2003. Lisbon 1755: A case of triggered onshore rupture?. Bull. Seism. Soc. Am. 93: 2056-2068.

Wells, D., and Coppersmith, K., 1994. New empirical relationships among magnitude, rupture length, rupture width, rupture area and surface displacement. Bull. Seism. Soc. Am. 84, 974-1002.

Zitellini, N., et al., 2001. Source of 1755 Lisbon earthquake and tsunami investigated. Eos (Transactions, American Geophysical Union) 82, 285-291.

Zitellini, N., Rovere, M., Terrinha, P., Chierici, F., Matias, L., and BIGSETS Team 2004. Neogene through Quaternary tectonic reactivation of SW Iberian passive margin. Pure Appl. Geophys. 161, 565-587.

Zitellini, N., Gracia, E., Matias, L., Terrinha, P., Abreu, M.A., DeAlteriis, G., Henriet, J.P., Danobeitia, JJ., Masson, D., Mulder, T., Ramella, R., Somoza, L., and Diez, S., 2009. The quest for NWAfrica-SW Eurasia plate boundary west of Gibraltar. Earth Planet. Sci. Lett. v. 280, p. 13-50, doi :10.1016/j.epsl.2008.12.005.